

## PM<sub>2.5</sub> chemical composition and spatiotemporal variability during the California Regional PM<sub>10</sub>/PM<sub>2.5</sub> Air Quality Study (CRPAQS)

Judith C. Chow,<sup>1</sup> L.-W. Antony Chen,<sup>1</sup> John G. Watson,<sup>1</sup> Douglas H. Lowenthal,<sup>1</sup> Karen A. Magliano,<sup>2</sup> Kasia Turkiewicz,<sup>2</sup> and Donald E. Lehrman<sup>3</sup>

Received 1 July 2005; revised 7 December 2005; accepted 4 January 2006; published 25 May 2006.

[1] The 14-month-long (December 1999 to February 2001) Central California Regional PM<sub>10</sub>/PM<sub>2.5</sub> Air Quality Study (CRPAQS) consisted of acquiring speciated PM<sub>2.5</sub> measurements at 38 sites representing urban, rural, and boundary environments in the San Joaquin Valley air basin. The study's goal was to understand the development of widespread pollution episodes by examining the spatial variability of PM<sub>2.5</sub>, ammonium nitrate (NH<sub>4</sub>NO<sub>3</sub>), and carbonaceous material on annual, seasonal, and episodic timescales. It was found that PM<sub>2.5</sub> and NH<sub>4</sub>NO<sub>3</sub> concentrations decrease rapidly as altitude increases, confirming that topography influences the ventilation and transport of pollutants. High PM<sub>2.5</sub> levels from November 2000 to January 2001 contributed to 50–75% of annual average concentrations. Contributions from organic matter differed substantially between urban and rural areas. Winter meteorology and intensive residential wood combustion are likely key factors for the winter-nonwinter and urban-rural contrasts that were observed. Short-duration measurements during the intensive operating periods confirm the role of upper air currents on valley-wide transport of NH<sub>4</sub>NO<sub>3</sub>. Zones of representation for PM<sub>2.5</sub> varied from 5 to 10 km for the urban Fresno and Bakersfield sites, and increased to 15–20 km for the boundary and rural sites. Secondary NH<sub>4</sub>NO<sub>3</sub> occurred region-wide during winter, spreading over a much wider geographical zone than carbonaceous aerosol.

**Citation:** Chow, J. C., L.-W. A. Chen, J. G. Watson, D. H. Lowenthal, K. A. Magliano, K. Turkiewicz, and D. E. Lehrman (2006), PM<sub>2.5</sub> chemical composition and spatiotemporal variability during the California Regional PM<sub>10</sub>/PM<sub>2.5</sub> Air Quality Study (CRPAQS), *J. Geophys. Res.*, 111, D10S04, doi:10.1029/2005JD006457.

### 1. Introduction

[2] The California Regional PM<sub>10</sub>/PM<sub>2.5</sub> Air Quality Study (CRPAQS) was undertaken with an overall goal of understanding the causes of excessive PM (particulate matter) levels and to evaluate means to reduce them in central California and its major geographical feature, the San Joaquin Valley (SJV) [Watson *et al.*, 1998]. The SJV represents one of the largest PM<sub>2.5</sub> and PM<sub>10</sub> nonattainment areas in the United States (PM<sub>2.5</sub> and PM<sub>10</sub> are particles with aerodynamic diameters less than 2.5 and 10 micrometers [μm], respectively). It was expected that considerable variability in emissions, meteorology, and terrain in the SJV would translate into substantial differences in PM concentration and composition across the region. Knowledge of these spatiotemporal distributions of PM and its chemical constituents is essential for understanding source-receptor relationships and chemical, physical, and meteorological processes that cause elevated PM levels in the SJV.

[3] The SJV air basin is bordered on the west by the coastal mountain ranges and on the east by the Sierra Nevada range. These ranges converge at the Tehachapi Mountains at the southern end of the basin, ~200 km south of Fresno (the largest population center within ~150 km along a north-south line of the basin). Weather changes seasonally. Spring often brings weak, fast moving frontal passages characterized by low moisture content and high wind speeds. Summer meteorology is driven by heating, which creates a thermal low-pressure system and a large onshore pressure gradient between the coast and the desert. Fall and winter are influenced by the Great Basin High, with prolonged periods of air mass stagnation and limited vertical mixing. Morning mixing depths are shallow and ventilation rates are low during all seasons. Wind speeds are low throughout the day during winter in the absence of storm systems. Relative humidity (RH) is highest in winter and lowest in summer and fall.

[4] Central California emission source categories include (1) small- to medium-sized point sources (e.g., power stations, natural gas boilers, steam generators, incinerators, and cement plants); (2) area sources (e.g., resuspended dust, petroleum extraction operations, cooking, wildfires, and residential wood combustion [RWC]); (3) mobile sources (e.g., cars, trucks, off-road heavy equipment, trains, and aircraft); (4) agricultural and ranching activities (e.g., tilling, fertilizers, herbicides, and livestock); and (5) bio-

<sup>1</sup>Division of Atmospheric Sciences, Desert Research Institute, Reno, Nevada, USA.

<sup>2</sup>California Air Resources Board, Sacramento, California, USA.

<sup>3</sup>Technical and Business Systems, Santa Rosa, California, USA.

genic sources (e.g., nitrogen oxides [NO<sub>x</sub>] from biological activity in soils and hydrocarbon emissions from plants). Agriculture is the main industry in the valley, where the major crops are cotton, alfalfa, corn, safflower, grapes, and tomatoes. Cattle feedlots and dairies constitute most of the animal husbandry in the region, along with chicken and turkey farms, which are major sources of ammonia (NH<sub>3</sub>) emissions.

[5] Past studies [Chow *et al.*, 1992, 1993a, 1996, 1998] have shown that elevated PM concentrations frequently occur in winter, when PM<sub>10</sub> concentrations are primarily in the PM<sub>2.5</sub> size fraction. Chemical mass balance receptor models [Magliano *et al.*, 1999; Schauer and Cass, 2000] have attributed winter PM episodes in urban areas to RWC emissions, motor vehicle exhaust, and secondary ammonium nitrate (NH<sub>4</sub>NO<sub>3</sub>). NH<sub>4</sub>NO<sub>3</sub> generally accounted for 30–60% of PM<sub>2.5</sub> during winter [Magliano *et al.*, 1998a, 1998b, 1999; Chow *et al.*, 1999]. Vehicular exhaust and RWC emissions are mostly in the PM<sub>2.5</sub> fraction with abundant organic carbon (OC) and elemental carbon (EC).

[6] Watson and Chow [2002a] developed a conceptual model that describes the interplay of emissions and meteorology leading to transport of pollutants and formation of widespread PM<sub>2.5</sub> episodes across the SJV in winter. The model begins with a shallow radiation surface inversion (100–200 m deep) which is decoupled from a valley-wide mixed layer aloft between ~1700 local time (LT) and ~1100 LT the next morning. At night, the cities experience a build up of primary pollutants emitted from traffic and RWC. Nitric acid (HNO<sub>3</sub>) can form in the upper layer during nighttime hours through a series of reactions [Atkinson *et al.*, 1986; Stockwell *et al.*, 2000; Pun and Seigneur, 2001]. Prevented from deposition by the surface inversion, this HNO<sub>3</sub> would be made available over rural areas with high NH<sub>3</sub> emissions to rapidly create NH<sub>4</sub>NO<sub>3</sub>. Limited upper air observations [Lehrman *et al.*, 1998] indicate that winds within the valley-wide layer often reach speeds of 1–6 m s<sup>-1</sup> while surface winds are <1 m s<sup>-1</sup>. This implies that secondary NH<sub>4</sub>NO<sub>3</sub> can be mixed throughout the valley in one to two days. When radiative heating breaks the inversion after ~1100 LT, turbulent mixing between the upper and surface layers intensifies, causing a net downward flux of NH<sub>4</sub>NO<sub>3</sub>, which escalates near the surface. In urban areas, this mixing also dilutes the concentrations of primary pollutants, creating a complex diurnal pattern of PM<sub>2.5</sub> [Watson *et al.*, 2002].

[7] This paper (1) statistically summarizes CRPAQS PM<sub>2.5</sub> mass and chemical compositions, (2) investigates chemical closure for PM<sub>2.5</sub> mass, (3) analyzes the spatio-temporal variability of PM<sub>2.5</sub> and its chemical composition, (4) examines episodes of elevated PM<sub>2.5</sub> during winter in the context of the conceptual model of Watson and Chow [2002a], and (5) evaluates the zones of representation for PM<sub>2.5</sub> sampling sites and their implications for future air quality monitoring and research.

## 2. Ambient Network

[8] The CRPAQS set up a PM<sub>2.5</sub> network consisting of 38 sites (Figure 1) where ambient measurements were acquired for 14 months. This network covered the SJV and surrounding air basins (i.e., San Francisco Bay, Sacramento Valley,

Mountain Counties, Great Basin Valleys, and Mojave Desert), and sampled urban, suburban, regional, transport, and rural background environments. The entire network covered a region ~600 km long by 200 km wide (Figure 1). Sampling took place from 2 December 1999 through 3 February 2001, including an annual program between 1 February 2000 and 31 January 2001. Sampling was also conducted during “Winter Intensive Operating Periods (IOPs),” which were selected on the basis of forecasts of high PM<sub>2.5</sub> between 15 December 2000 and 3 February 2001. The annual program included every sixth day 24-hour sampling at three anchor sites (Fresno Supersite (FSF [Watson *et al.*, 2000]), Angiola (ANGI), and Bakersfield (BAC)) and at 35 satellite sites (Table 1). Winter IOPs included five times/day 3–8 hour samples for 15 days at the five anchor sites (Bethel Island (BTI), Sierra Nevada Foothills (SNFH), FSF, ANGI, and BAC) and daily 24-hour sampling for 13 days at 25 satellite sites.

[9] The FSF and BAC sites represented the two major urban centers in the SJV. ANGI, located between these two urban centers, was chosen to represent regional transport and/or pollutant gradients. BTI and SNFH operated during winter IOPs were intended to represent interbasin gradient and transport boundary conditions. Both were also satellite sites during the annual program. BTI is located at the northwest corner of the SJV ~50 km east of San Francisco. SNFH (589 m above mean sea level [MSL]) is located on the upslope of the western Sierra Nevada approximately at the same latitude as FSF. The 38 sites were categorized into eight site types depending on the type of land use and surrounding environs (Table 1). These included eighteen community exposure sites, eleven emissions source-dominated sites, nine visibility sites, eleven intrabasin gradient sites, two vertical gradient sites, one intrabasin transport site, six interbasin transport sites, and seven boundary/background sites. These were nominal classifications made during the study design, and it was later found that several sites represented different environments at different times of the year.

[10] At each of the anchor sites, a Desert Research Institute (DRI, Reno, NV, USA) sequential filter sampler (SFS) [Chow *et al.*, 1994, 1996; Chen *et al.*, 2002] collected PM<sub>2.5</sub> through two sampling channels (20 liters per minute [L min<sup>-1</sup>]). Details of the sampling system and filter pack configuration are documented in Table 1 footnotes. The backup sodium chloride (NaCl)-impregnated cellulose-fiber filter collected nitrate (NO<sub>3</sub><sup>-</sup>) volatilized from the quartz-fiber filter to evaluate the negative bias for particulate NO<sub>3</sub><sup>-</sup> measurements [Zhang and McMurry, 1992; Hering and Cass, 1999; Chow *et al.*, 2005b]. The degree of NH<sub>4</sub>NO<sub>3</sub> evaporation from the front quartz-fiber filter depends on the temperature, relative levels of gaseous NH<sub>3</sub>, HNO<sub>3</sub>, particulate NH<sub>4</sub>NO<sub>3</sub> in the ambient air, and the fraction of gaseous species removed (denuded) in the sampling stream. Ashbaugh *et al.* [2004] reported that the inlet of a non-denuded IMPROVE sampler removed HNO<sub>3</sub> as effectively as an IMPROVE sampler with a HNO<sub>3</sub> denuder. In this paper, pNO<sub>3</sub><sup>-</sup> (total particulate NO<sub>3</sub><sup>-</sup>) represents the sum of nonvolatilized NO<sub>3</sub><sup>-</sup> from the front filter and volatilized NO<sub>3</sub><sup>-</sup> from the backup filter. Two sequential gas samplers (SGSs [Chow *et al.*, 1996; Chen *et al.*, 2002]) at the five anchor sites during the winter IOPs quantified gaseous NH<sub>3</sub>

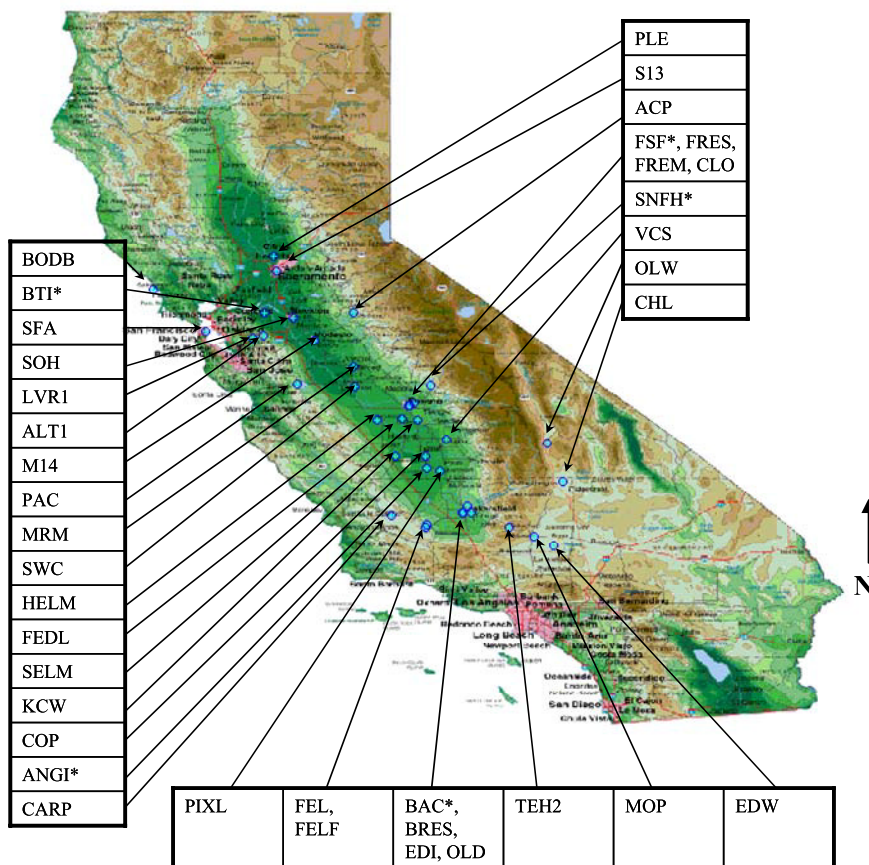


**Figure 1.** The 24-hour average speciated ambient PM<sub>2.5</sub> network at five anchor sites (denoted by asterisks) and 35 satellite sites during CRPAQS.

and HNO<sub>3</sub> using the denuder difference method [Chow *et al.*, 1993b].

[11] PM<sub>2.5</sub> MiniVol samplers (AirMetrics, Springfield, Oregon, USA) that were used at the satellite sites yield mass concentrations comparable to PM<sub>2.5</sub> Federal Reference Method (FRM) compliance samplers [Baldauf *et al.*, 2001; Chow *et al.*, 2005b]. Occasional malfunctions of batteries and pumps resulted in missing data. The satellite network had a valid data capture rate in excess of 80% over the study period with the exception of the dairy site (FEDL; 62%), the Edwards site (EDW; 77%), and the Bakersfield residential site (BRES; 66%) (Table 2). Since the missing data occurred randomly in time, they are not expected to bias the annual averages.

[12] Uncertainty was determined for each measurement on the basis of (1) sample volume uncertainty, based on flow rate performance tests; (2) replicate precision from the chemical analyses; and (3) the uncertainty of the dynamic field blank, which is the larger of the standard deviation of the individual blank values or their root-mean-squared analytical uncertainty. The valley-wide average blank concentrations for PM<sub>2.5</sub> mass, nonvolatilized NO<sub>3</sub><sup>-</sup>, volatilized NO<sub>3</sub><sup>-</sup>, OC, EC, and NH<sub>3</sub> were 2.1 ± 1.2, 0.1 ± 0.1, 0.01 ± 0.04, 3.1 ± 1.3, 0.2 ± 0.3, and 0.9 ± 0.5 μg m<sup>-3</sup>, respectively. Ambient concentrations reported for CRPAQS are blank subtracted [e.g., Watson *et al.*, 1995]. For mass, NO<sub>3</sub><sup>-</sup>, ammonium (NH<sub>4</sub><sup>+</sup>), and total carbon (TC = OC + EC), the uncertainty was typically within ±10% for measured values exceeding 10 times the minimum detection level

(MDL). Measured NO<sub>3</sub><sup>-</sup> and sulfate (SO<sub>4</sub><sup>2-</sup>) were compared to NH<sub>4</sub><sup>+</sup> as part of the data validation process. The high correlation ( $R^2 \sim 0.99$ ) between the anions and cations, and a nearly 1:1 molar ratio, indicates that the dominant form of NH<sub>4</sub><sup>+</sup> was NH<sub>4</sub>NO<sub>3</sub>. Only ~9% of NH<sub>4</sub><sup>+</sup> was associated with other anions, mainly SO<sub>4</sub><sup>2-</sup>. Hereafter, the concentration of front quartz-filter NH<sub>4</sub>NO<sub>3</sub> is estimated as  $1.29 \times [\text{NO}_3^-]$  (and pNH<sub>4</sub>NO<sub>3</sub> as  $1.29 \times [\text{pNO}_3^-]$ ). In addition to the CRPAQS network, PM<sub>2.5</sub> and PM<sub>10</sub> mass measurements were acquired with FRMs at compliance sites in cities and at IMPROVE sites in central California's Class I areas. Some of these were collocated with CRPAQS measurements [Chow *et al.*, 2006a].

### 3. Spatiotemporal Variations of PM<sub>2.5</sub>

[13] Annual-average PM<sub>2.5</sub>, based on four quarterly averages (i.e., calendar quarter [see U.S. Environmental Protection Agency (U.S. EPA), 1997]) at 14 of the 38 CRPAQS sites, exceeded the U.S. annual PM<sub>2.5</sub> National Ambient Air Quality Standard (NAAQS) of 15 μg m<sup>-3</sup> (Table 2). Most of these exceedances occurred in the southern SJV at urban sites such as FSF (23 μg m<sup>-3</sup>), Visalia (VCS; 22 μg m<sup>-3</sup>), and BAC (26 μg m<sup>-3</sup>), and also at the regional transport ANGI site (18.7 μg m<sup>-3</sup>). These averages differ from every sixth day arithmetic means from the annual program by <10%, except at BRES. This corroborates the limited influence of missing data on the annual averages. The

Table 1. Summary of CRPAQS Aerosol Measurements at the Anchor and Satellite Sites

Site Code	Site Name	Site Location	Site Type/Characteristics	Longitude	Latitude	Elevation, m	Anchor Sites, <sup>a</sup> Sampling Period			Satellite Sites <sup>b</sup>			
							Annual	Winter Intensive	T/C	Filter Pack, PM <sub>2.5</sub>	q/n	Annual	Winter Intensive
ACP	Angels Camp	elevated rural; 6850 Studhorse Flat Road, Sonora	intrabasin gradient	-120.491	38.006	373		FTC <sup>c</sup>	FQN <sup>d</sup>	X		X	
ALTI	Altamont Pass	elevated rural; Flynn Road exit, I-580	interbasin transport	-121.660	37.718	350		FTC		X		X	
ANGI	Angiola-ground level	rural; 36078 4th Avenue, Corcoran	intrabasin gradient/transport, vertical gradient, visibility	-119.538	35.948	60	X						
BAC	Bakersfield-5558 California Street	urban; 5558 CA Ave. #430 (STI) #460 (ARB), Bakersfield	community exposure, visibility	-119.063	35.357	119	X						
BODG	Bodega Marine Lab	marine; Bodega Marine Lab, 2099 Westside Road, Bodega Bay	boundary/background	-123.073	38.319	17		FTC	FQN	X		X	
BRES	BAC-residential	urban; 7301 Remington Avenue, Bakersfield	source: wood burning	-119.084	35.358	117		FTC	FQN	X		X	
BTI	Bethel Island	rural; 5551 Bethel Island Road, Bethel Island	interbasin transport	-121.642	38.006	2	X	FTC	FQN	X			
CARP	Carrizo Plain	elevated rural; Soda Springs Road, 0.5 mile south of California Valley	intrabasin gradient, visibility	-119.996	35.314	598		FTC		X			
CHL	China Lake	elevated rural; Baker site	visibility	-117.776	35.774	684		FTC	FQN	X			
CLO	Clovis	suburban; 908 N. Villa, Clovis	community exposure	-119.716	36.819	108		FTC	FQN	X		X	
COP	Corcoran-Patterson Avenue	rural; 1520 Patterson Ave., Corcoran	community exposure	-119.566	36.102	63		FTC	FQN	(X) <sup>e</sup>		X	
EDI	Edison	urban; 4101 Kimber Avenue, Bakersfield	intrabasin gradient	-118.957	35.350	118		FTC		X		X	
EDW	Edwards Air Force Base	elevated rural; north end of Rawinsonde Road, Edwards AFB	intrabasin gradient, visibility	-117.904	34.929	724		FTC	FQN	X			
FEDL	feedlot or dairy	rural; 8555 S. Valentine, Fresno (near Raisin City)	source: cattle	-119.855	36.611	76		FTC	FQN	X		X	
FEL	Fellows	elevated rural; across from 25883 Hwy 33, Fellows	source: oilfields	-119.546	35.203	359		FTC	FQN	X		X	
FELF	foothills above Fellows	elevated rural; Texaco Pump Site 47-1, Fellows	intrabasin gradient	-119.557	35.171	512		FTC	FQN	X		X	
FREM	Fresno MV	urban; Pole # 16629, 2253 E. Shields Ave., Fresno	source: motor vehicle	-119.783	36.780	96		FTC	FQN	X		X	
FRES	residential area near FSF, with wood burning	urban; Pole # 16962, 3534 Virginia Lane, Fresno	source: wood burning	-119.768	36.783	97		FTC	FQN	(X)		X	
FSF	Fresno-3425 First Street	urban; 3425 First Street, Fresno	community exposure, visibility	-119.773	36.782	97	X						
HELM	agricultural fields/Helm-central Fresno County	rural; near Placer and Springfield	intrabasin gradient	-120.177	36.591	55		FTC	FQN	X		X	
KCW	Kettleman City	rural; Omaha Avenue 2 miles west of Hwy 41, Kettleman City	intrabasin gradient	-119.948	36.095	69		FTC		X		X	
LVR1	Livermore - new site	rural; 793 Rincon Street, Livermore	interbasin transport	-121.784	37.688	138		FTC	FQN	X		X	
M14	Modesto 14th St.	urban; 814 14th Street, Modesto	community exposure	-120.994	37.642	28		FTC	FQN	(X)		X	
MOP	Mojave-Poole	elevated rural; 923 Poole Street, Mojave	community exposure	-118.148	35.051	832		FTC	FQN	X		X	
MRM	Merced-midtown	suburban; 2334 M Street, Merced	community exposure	-120.481	37.308	53		FTC	FQN	X		X	

Table 1. (continued)

Site Code	Site Name	Site Location	Site Type/Characteristics	Longitude	Latitude	Elevation, m	Anchor Sites, <sup>a</sup> Sampling Period		Filter Pack, PM <sub>2.5</sub>		Satellite Sites <sup>b</sup> Sampling Period	
							Annual	Winter Intensive	T/C	q/n	Annual	Winter Intensive
OLD	Oildale-Manor	suburban; 3311 Manor Street, Oildale	community exposure	-119.017	35.438	180		FTC	FQN		FQN	(X)
OLW	Olancho	elevated rural; just to east of Hwy 395	background	-117.993	36.268	1124		FTC	FQN		FQN	X
PAC	Pacheco Pass	elevated rural; Upper Cottonwood Wildlife Area, west of Los Banos	interbasin transport	-121.222	37.073	452		FTC				X
PIXL	Pixley Wildlife Refuge	rural; Road 88, 1.5 miles north of Avenue 56, Alpaugh	rural, intrabasin gradient	-119.376	35.914	69		FTC	FQN		FQN	X
PLE	Pleasant Grove (north of Sacramento)	rural; 7310 Pacific Avenue, Pleasant Grove	intrabasin gradient	-121.519	38.766	10		FTC	FQN		FQN	X
S13	Sacramento-1309 T Street	urban; 1309 T Street, Sacramento	community exposure	-121.493	38.568	6		FTC	FQN		FQN	X
SELM	Selma (south Fresno area gradient site)	rural; 7225 Huntsman Avenue, Selma	community exposure	-119.660	36.583	94		FTC	FQN		FQN	X
SFA	San Francisco - Arkansas	marine/urban; 10 Arkansas St., San Francisco	community exposure	-122.399	37.766	6		FTC	FQN		FQN	X
SNFH	Sierra Nevada Foothills	elevated rural; 31955 Auberry Road, Auberry	vertical gradient, intrabasin gradient, visibility	-119.496	37.063	589		FTC	FQN		FQN	X
SOH	Stockton-Hazleton	urban; 1601 E. Hazleton, Stockton	intrabasin gradient	-121.269	37.950	8		FTC	FQN		FQN	X
SWC	SW Chowchilla	rural; 20513 Road 4, Chowchilla	interbasin transport	-120.472	37.048	43		FTC	FQN		FQN	X
TEH2	Tehachapi Pass	elevated rural; Near 19805 Dovetail Court, Tehachapi	interbasin transport, visibility	-118.482	35.168	1229		FTC				X
VCS	Visalia Church St.	urban; 310 Church Street, Visalia	community exposure	-119.291	36.333	102		FTC	FQN		FQN	(X)
Total number of sites								3	5	35	29	35

<sup>a</sup>Anchor site annual sampling program used DRI medium-volume sequential filter samplers (SFS) equipped with Bendix 240 cyclone (Clearwater, Florida, USA) PM<sub>2.5</sub> inlets and preceding nitric acid (HNO<sub>3</sub>) denuder, consisting of anodized aluminum tubes coated with aluminum oxide [Chow *et al.*, 1993b]. The denuders remove HNO<sub>3</sub> with an efficiency of >90% [Chow *et al.*, 2005a]. Sampling was conducted daily, 24 hours/day (midnight to midnight) from 2 December 1999 to 3 February 2001 at a flow rate of 20 L min<sup>-1</sup>. Two filter packs were used for sampling. (1) Each Teflon/citric acid filter pack (FTC) consists of a front Teflon-membrane filter (#R2P1047, Pall Corp, Putnam, Connecticut, USA) for mass, b<sub>abs</sub>, and elemental analyses, backed up by a citric-acid-impregnated cellulose-fiber filter (31ET, Whatman, Brentford, Middlesex, U.K.) for ammonia (NH<sub>3</sub>), and (2) each quartz/sodium chloride (NaCl) filter pack (FQN) consists of a front quartz-fiber filter (#2500QAT-UP, Pall Corp, Putnam, Connecticut, USA) for ion and carbon analyses, backed up by an NaCl-impregnated cellulose-fiber filter for volatilized nitrate.

<sup>b</sup>Anchor site winter intensive sampling included both SFS for PM<sub>2.5</sub> sampling and sequential gas samplers (SGS) for NH<sub>3</sub> and HNO<sub>3</sub> sampling by denuder difference on 15 forecast episode days (IOP\_1: 15 December 2000 to 18 December 2000, IOP\_2: 26 December 2000 to 28 December 2000, IOP\_3: 4 January 2001 to 7 January 2001, and IOP\_4: 31 January 2001 to 3 February 2001). The two SGS were equipped with (1) citric-acid-coated glass denuders and quartz-fiber filters backed up by citric-acid-impregnated cellulose-fiber filters for NH<sub>3</sub>, and (2) anodized aluminum denuders and quartz-fiber filters backed up by sodium-chloride-impregnated cellulose-fiber filters for HNO<sub>3</sub>.

<sup>c</sup>FTC filter pack: Teflon-membrane filter samples were analyzed for mass by gravimetry (for filters equilibrated at 21 ± 1.5°C and 35 ± 5%), filter light transmission (b<sub>abs</sub>) by densitometry, and elements (Na, Mg, Al, Si, P, S, Cl, K, Ca, Ti, V, Cr, Mn, Fe, Co, Ni, Cu, Zn, Ga, As, Se, Br, Rb, Sr, Y, Zr, Mo, Pd, Ag, Cd, In, Sn, Sb, Ba, La, Au, Hg, Tl, Pb, and U) by x-ray fluorescence (XRF [Watson *et al.*, 1998]); quartz-fiber filter samples were analyzed for anions (chloride [Cl<sup>-</sup>], nitrate [NO<sub>3</sub><sup>-</sup>], sulfate [SO<sub>4</sub><sup>2-</sup>]) by ion chromatography [Chow and Watson, 1999], ammonium (NH<sub>4</sub><sup>+</sup>) by automated colorimetry, water-soluble sodium (Na<sup>+</sup>) and potassium (K<sup>+</sup>) by atomic absorption spectrophotometry, and 7-fraction organic and elemental carbon (OC) combusted at 120°C, OC2 at 250°C, OC3 at 450°C, OC4 at 550°C, EC1 at 550°C, EC2 at 700°C, and EC3 at 800°C with pyrolysis correction) by thermal/optical reflectance (TOR) following the Interagency Monitoring of Protected Visual Environments (IMPROVE) protocol [Chow *et al.*, 1993c, 2001, 2004, 2005a; Chen *et al.*, 2004; Watson *et al.*, 1994]; citric-acid-impregnated filter samples were analyzed for NH<sub>3</sub> by automated colorimetry; and NaCl-impregnated filters were analyzed for volatilized nitrate by ion chromatography.

<sup>d</sup>Used battery-powered MiniVol samplers (Airmetrics, Eugene, Oregon) equipped with PM<sub>10</sub>/PM<sub>2.5</sub> (in tandem) or PM<sub>10</sub> inlets at a flow rate of 5 L min<sup>-1</sup>. Filter pack assembly for PM<sub>2.5</sub> followed the same FTC and FQN configurations of those at the anchor sites, with mass, elements, and NH<sub>3</sub> acquired at all 35 sites. Carbon, ions, and volatilized NO<sub>3</sub><sup>-</sup> were acquired at 29 sites.

<sup>e</sup>Parentheses indicate that the site includes the PM<sub>10</sub> sites operated during the annual program.

**Table 2.** Summary of PM<sub>2.5</sub> Mass and Chemical Composition at 38 Sites During CRPAQS<sup>a</sup>

Site	14-Month <sup>b/</sup> Annual <sup>c</sup>				Annual Means From				Maximum PM <sub>2.5</sub> , <sup>d</sup> $\mu\text{g m}^{-3}$	Date	Annual				Annual Reconstructed						
	Valid Measurements	Spring Mean PM <sub>2.5</sub> , <sup>e</sup> $\mu\text{g m}^{-3}$	Summer Mean PM <sub>2.5</sub> , <sup>d</sup> $\mu\text{g m}^{-3}$	Fall Mean PM <sub>2.5</sub> , <sup>e</sup> $\mu\text{g m}^{-3}$	Winter Mean PM <sub>2.5</sub> , <sup>e</sup> $\mu\text{g m}^{-3}$	Annual Mean PM <sub>2.5</sub> , <sup>b</sup> $\mu\text{g m}^{-3}$	14-Month Mean PM <sub>2.5</sub> , <sup>b</sup> $\mu\text{g m}^{-3}$	Maximum PM <sub>2.5</sub> , <sup>d</sup> $\mu\text{g m}^{-3}$			Annual NH <sub>4</sub> NO <sub>3</sub> (Front), <sup>i</sup> $\mu\text{g m}^{-3}$	Annual NH <sub>4</sub> NO <sub>3</sub> (Back), <sup>j</sup> $\mu\text{g m}^{-3}$	Annual OM, <sup>k</sup> $\mu\text{g m}^{-3}$	Annual EC, (NH <sub>2</sub> ) <sub>2</sub> SO <sub>4</sub> , <sup>l</sup> $\mu\text{g m}^{-3}$	Annual Crustal, <sup>m</sup> $\mu\text{g m}^{-3}$	Annual PM <sub>2.5</sub> Mass, <sup>n</sup> $\mu\text{g m}^{-3}$	Annual PM <sub>2.5</sub> Mass Closure, <sup>o</sup> %				
ACP	72/61	3.9 ± 2.1	3.6 ± 1.6	3.6 ± 2.2	5.0 ± 5.4	3.4 ± 2.1	4.2 ± 3.6	18.9	1/7/2000	3.5	3.4	25.5	1.0	0.1	3.8	0.9	1.1	0.4	7.6	223	
ALTI	68/61	4.2 ± 1.8	5.1 ± 2.6	6.1 ± 10.2	13.3 ± 18.7	7.2	7.3 ± 11.7	71.7	1/7/2001	16.8	3.9	58.6	...	...	...	...	...	0.3	...	...	
ANGI	55/50	10.9 ± 3.9	11.4 ± 5.6	20.6 ± 26.7	29.1 ± 23.0	18.7	19.1 ± 23.7	123.4	1/7/2001	41.4	11.3	55.0	8.1	1.5	5.3	0.8	2.0	3.0	19.6	103	
BAC	66/57	19.8 ± 12.8	13.3 ± 2.9	23.2 ± 22.0	43.5 ± 36.7	26.0	27.0 ± 27.5	132.7	1/1/2001	56.9	15.3	55.4	9.8	2.4	9.9	2.0	2.6	3.4	28.3	105	
BODG	67/57	10.5 ± 4.9	4.6 ± 4.1	5.5 ± 4.3	14.8 ± 9.8	8.9	10.0 ± 8.1	35.3	1/19/2001	13.6	7.9	36.3	1.6	0.1	1.6	0.4	1.9	0.2	10.2	110	
BRES	45/40	7.9 ± 3.1	7.6 ± 2.5	20.1 ± 27.6	53.6 ± 42.1	43.7	27.9 ± 36.5	158.9	1/1/2001	59.1	7.1	73.5	10.4	1.0	10.0	2.8	2.1	1.4	27.4	98	
BTI	72/61	4.1 ± 1.9	4.5 ± 2.9	7.0 ± 11.8	18.0 ± 19.2	8.8	8.0 ± 13.9	10.0 ± 14.2	76.6	1/7/2001	22.8	3.9	65.8	3.5	0.1	4.1	1.3	1.7	0.7	12.2	137
CARP	63/63	4.2 ± 2.3	3.4 ± 2.2	7.5 ± 8.1	8.3 ± 10.0	5.5	6.0 ± 7.0	32.6	1/19/2001	11.8	3.9	50.4	...	...	...	...	...	0.9	...	...	
CHL	60/51	2.1 ± 1.3	3.3 ± 2.5	1.4 ± 1.4	5.6 ± 16.4	1.7	1.9 ± 1.8	3.4 ± 9.8	74.5	1/7/2000	0.8	2.4	9.9	0.4	0.2	4.1	0.8	1.0	0.4	7.1	375
CLO	66/56	7.8 ± 3.4	8.6 ± 2.5	21.4 ± 31.0	47.0 ± 38.2	20.6	20.8 ± 27.8	25.3 ± 32.0	130.1	1/1/2001	55.6	9.1	67.0	7.8	0.8	9.6	2.5	1.9	1.2	23.5	113
COP	71/60	10.0 ± 7.0	8.0 ± 1.7	20.0 ± 19.2	37.8 ± 35.7	17.9	18.2 ± 22.6	21.9 ± 26.5	124.7	1/7/2001	42.3	9.4	59.9	8.7	0.7	7.2	1.7	2.0	1.6	21.8	120
EDI	64/55	10.0 ± 5.7	10.5 ± 3.3	32.2 ± 43.8	38.3 ± 40.0	24.9	24.5 ± 34.5	24.9 ± 33.2	160.8	1/1/2001	48.0	14.8	51.9	...	...	...	...	...	3.1	...	...
EDW	50/47	4.5 ± 2.1	6.3 ± 1.3	5.0 ± 4.7	5.1 ± 4.9	5.0	5.3 ± 3.6	5.3 ± 3.7	16.9	9/21/2000	5.6	5.3	26.1	1.2	0.7	4.0	0.8	1.5	0.8	8.8	165
FEDL	38/38	...	27.8 ± 12.3	25.3 ± 15.3	38.6 ± 32.7	28.8	29.9 ± 21.3	29.9 ± 21.3	115.7	1/7/2001	38.4	23.7	35.0	10.6	0.2	9.7	1.9	2.3	3.4	29.0	97
FEL	71/61	7.5 ± 6.9	5.4 ± 1.5	13.4 ± 19.2	20.1 ± 20.6	12.2	12.2 ± 16.4	12.7 ± 16.4	74.2	1/1/2001	30.0	5.9	63.0	5.4	0.8	5.5	1.1	2.1	1.2	15.9	131
FELF	70/60	5.1 ± 2.8	4.9 ± 1.7	13.2 ± 18.1	19.6 ± 18.3	11.6	11.6 ± 15.4	12.0 ± 15.1	69.4	1/1/2001	29.5	5.1	65.8	6.5	0.7	5.2	0.9	2.2	0.6	15.9	137
FREM	67/60	9.7 ± 3.6	9.1 ± 2.9	21.8 ± 27.2	56.5 ± 47.7	24.8	25.3 ± 35.2	27.6 ± 36.3	176.0	1/1/2001	67.6	9.9	69.5	8.1	0.8	13.9	3.7	2.0	1.2	29.7	118
FRES	66/57	9.0 ± 3.9	7.8 ± 2.7	21.2 ± 27.0	55.9 ± 46.5	22.8	24.2 ± 33.9	28.4 ± 37.0	169.4	1/1/2001	63.3	8.9	70.3	7.6	0.8	11.7	2.9	1.9	0.8	25.7	106
FSF	71/60	11.2 ± 6.0	9.4 ± 2.9	20.1 ± 21.9	53.9 ± 41.5	23.3	23.7 ± 29.4	28.4 ± 33.4	148.3	1/1/2001	60.0	10.6	65.4	5.2	2.6	10.4	2.0	1.8	1.5	21.5	90
HELM	70/59	5.0 ± 2.0	5.5 ± 2.1	12.7 ± 15.5	25.9 ± 28.5	11.8	11.8 ± 16.3	14.4 ± 20.7	114.8	12/26/1999	30.8	5.3	66.1	6.5	0.7	5.0	1.4	1.8	0.8	16.2	138
KCW	64/55	6.1 ± 3.3	6.1 ± 2.2	13.9 ± 26.7	32.6 ± 32.7	10.9	12.9 ± 19.3	16.8 ± 25.3	112.7	1/7/2000	29.9	5.9	62.9	...	...	...	...	...	0.9	...	...
LXRI	72/61	6.2 ± 4.1	6.0 ± 3.6	8.7 ± 11.1	20.6 ± 22.3	10.5	10.6 ± 14.9	11.9 ± 15.8	95.4	1/7/2001	24.7	5.6	59.6	3.3	0.2	6.2	2.4	1.6	0.3	14.6	137
M4	71/60	6.1 ± 2.2	7.1 ± 5.1	16.0 ± 22.7	41.9 ± 34.4	17.3	17.3 ± 25.5	21.0 ± 27.7	136.1	1/7/2001	47.8	6.2	72.1	6.2	0.6	9.2	2.0	2.0	0.6	21.1	122
MOP	69/58	5.6 ± 3.6	5.3 ± 1.9	4.8 ± 3.8	2.8 ± 3.3	4.4	4.3 ± 3.3	4.4 ± 3.4	15.6	11/14/2000	2.9	4.8	16.6	1.0	0.5	5.0	1.1	1.4	0.6	9.5	219
MRM	72/61	7.0 ± 3.5	6.8 ± 3.3	13.0 ± 13.2	36.6 ± 28.3	13.9	14.0 ± 14.4	18.9 ± 22.5	115.9	12/20/1999	32.4	7.4	59.3	6.5	0.4	8.9	2.2	1.8	0.7	20.7	148
OLD	65/55	9.5 ± 5.7	7.6 ± 2.0	23.1 ± 26.8	40.9 ± 38.4	21.5	21.1 ± 29.0	23.5 ± 29.9	140.6	1/1/2001	52.6	8.2	68.3	11.0	1.0	9.0	0.9	2.6	1.3	26.3	125
OLW	65/54	3.1 ± 4.4	5.5 ± 5.9	1.5 ± 1.3	3.0 ± 3.9	3.2	3.1 ± 5.8	3.2 ± 5.6	39.2	7/29/2000	1.9	3.6	15.3	0.3	0.1	4.0	1.7	0.8	0.7	7.0	224
PAC	71/61	3.5 ± 2.1	2.9 ± 1.6	4.6 ± 8.3	14.2 ± 17.6	6.1	6.1 ± 9.2	7.4 ± 12.1	64.3	12/26/1999	15.0	2.9	62.9	...	...	...	...	...	0.1	...	...
PIXL	69/61	9.8 ± 6.7	10.0 ± 8.2	17.7 ± 14.5	38.6 ± 33.0	18.4	18.5 ± 21.5	21.2 ± 24.1	106.6	1/7/2001	42.9	9.8	59.4	9.9	0.4	6.0	1.6	2.2	1.3	21.6	117
PLE	70/59	6.4 ± 2.5	6.4 ± 2.5	9.1 ± 9.8	18.0 ± 18.0	9.1	9.1 ± 9.1	11.1 ± 12.7	66.3	12/20/1999	18.6	5.6	52.4	3.0	0.2	6.8	1.9	1.4	0.5	14.2	155
SELM	71/61	11.4 ± 7.3	8.9 ± 3.3	18.0 ± 16.5	41.2 ± 34.7	18.2	18.3 ± 19.4	22.8 ± 26.0	110.4	12/26/1999	40.3	10.5	56.1	8.3	0.8	7.8	2.3	2.2	1.1	22.5	122
SFA	72/61	8.0 ± 4.7	5.1 ± 3.7	9.0 ± 7.9	16.2 ± 14.7	9.2	9.2 ± 8.6	10.5 ± 10.8	63.4	12/26/1999	18.3	6.0	50.5	3.1	0.1	4.5	1.8	2.0	0.5	13.8	150
SNFH	70/60	6.3 ± 3.7	5.6 ± 1.8	8.0 ± 4.4	18.1 ± 18.6	8.5	8.5 ± 8.1	10.7 ± 12.6	70.2	1/1/2000	15.6	5.9	46.8	2.8	0.4	6.4	1.3	1.6	0.6	13.4	157
SOH	70/59	5.4 ± 2.3	7.2 ± 5.2	9.4 ± 9.0	31.1 ± 27.3	12.7	12.8 ± 16.5	16.1 ± 20.7	103.3	12/20/1999	32.8	6.0	64.7	4.8	0.6	7.2	2.2	1.9	0.6	17.9	140
SWC	70/59	7.4 ± 2.5	6.5 ± 2.2	13.7 ± 15.5	28.0 ± 28.7	13.1	12.9 ± 15.7	16.0 ± 20.9	97.4	12/26/1999	32.5	6.8	61.5	6.3	0.7	4.5	1.4	1.6	0.8	15.6	122
TEH2	64/53	9.1 ± 3.7	6.5 ± 2.7	7.4 ± 5.1	5.6 ± 8.9	7.3	7.3 ± 6.2	6.8 ± 6.2	35.4	12/8/2000	7.3	7.3	25.1	...	...	...	...	...	0.5	...	...
VCS	72/61	14.1 ± 8.7	9.5 ± 3.3	18.6 ± 18.1	46.9 ± 37.2	21.7	21.9 ± 24.7	25.9 ± 28.8	123.7	1/1/2001	50.3	11.8	58.7	9.5	0.8	9.8	2.4	2.3	1.3	26.5	121

<sup>a</sup>Anchor sites are coded in bold; refer to Table 1 for site codes.

<sup>b</sup>Consists of 72 every-6th-day sampling from 2 December 1999 to 3 February 2001.

<sup>c</sup>Consists of 61 every-6th-day sampling from 1 February 2000 to 31 January 2001 (CRPAQS annual period).

<sup>d</sup>Seasonal averages of spring (March to May), summer (June to August), fall (September to November), and winter (December to February) for the CRPAQS annual period.

<sup>e</sup>Arithmetic means of the four calendar quarters: January to March, April to June, July to September, and October to December during the CRPAQS annual period. January is from 2001 and the rest of the months are from 2000. Italics indicate <75% coverage in at least one quarter.

<sup>f</sup>Average of high PM<sub>2.5</sub> period (1 November 2000 to 31 January 2001).

<sup>g</sup>Average of low PM<sub>2.5</sub> period (1 February 2000 to 31 October 2000).

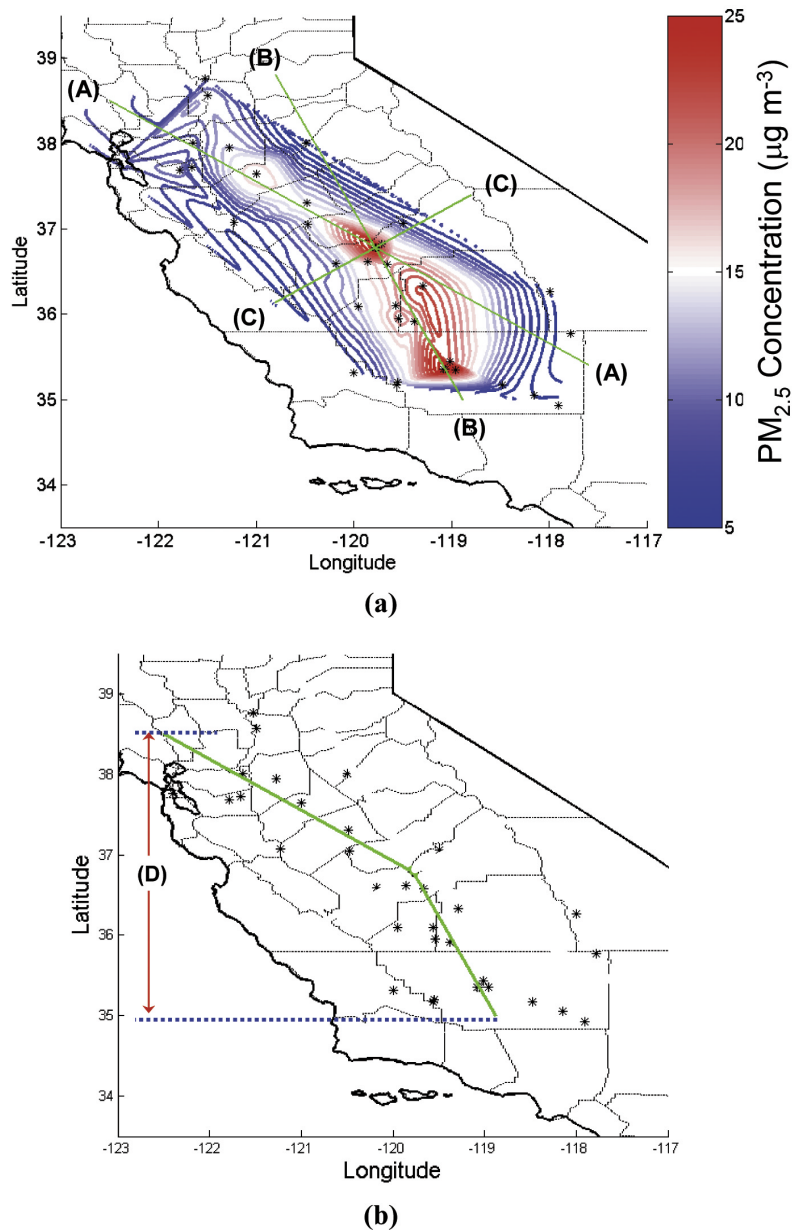


**Figure 2.** Spatial distribution of (a) annual PM<sub>2.5</sub> concentration (1 February 2000 to 31 January 2001) during CRPAQS and geographical cross sections A, B, and C and (b) the sampling sites and cross section D. Contours are determined with a two-dimensional cubic-spline algorithm using only sites with >70% valid measurements. The stars indicate locations of the sampling sites.

annual average determined by sixth day sampling is used in subsequent analyses rather than the annual average of quarterly averages required to determine NAAQS attainment.

[14] The PM<sub>2.5</sub> concentration decreased rapidly toward the higher-elevation valley boundary (Figure 2a). Three

sites in Bakersfield (residential BRES site, urban BAC site, and interbasin gradient Edison [EDI] site, all ~118 m above MSL) reported consistently high annual-average PM<sub>2.5</sub> concentrations of 24–28  $\mu\text{g m}^{-3}$ , despite the fact that each site represents different microenvironments. Tehachapi

*Notes to Table 2.*

$${}^h F_{high} = [C_{high} / (C_{high} + 3 \times C_{low})] \times 100.$$

$${}^i 1.29 \times ([\text{NO}_3^-]_{\text{FRONT}}).$$

$${}^j 1.29 \times ([\text{NO}_3^-]_{\text{BACKUP}}).$$

$${}^k 1.4 \times [\text{OC}].$$

$${}^l 1.38 \times [\text{SO}_4^{2-}].$$

$${}^m 2.2 \times [\text{Al}] + 2.49 \times [\text{Si}] + 1.63 \times [\text{Ca}] + 2.42 \times [\text{Fe}] + 1.94 \times [\text{Ti}].$$

${}^n \text{NH}_4\text{NO}_3$  (front filter, nonvolatilized  $\text{NH}_4\text{NO}_3$ ) + OM + EC +  $(\text{NH}_4)_2\text{SO}_4$  + crustal material (CM) + trace elements (other than geological material) and sea salt ( $\text{Na}^+$  +  $\text{Cl}^-$ ).

$${}^o (\text{Summed PM}_{2.5} \text{ mass/annual mean PM}_{2.5}) \times 100\%.$$

(TEH2), an interbasin transport site, located ~50 km to the southeast of EDI at 1229 m above MSL, recorded an annual-average PM<sub>2.5</sub> concentration of 7.3  $\mu\text{g m}^{-3}$ . The annual-average PM<sub>2.5</sub> concentration decreased further at the Mojave Desert (EDW; 724 m above MSL) and Mojave-Pool (MOP; 832 m above MSL) sites, averaging only 4.3–5.4  $\mu\text{g m}^{-3}$ . Similarly, annual-average PM<sub>2.5</sub> concentration decreased from 24  $\mu\text{g m}^{-3}$  at FSF, to 21  $\mu\text{g m}^{-3}$  at Clovis (CLO; 108 m above MSL, a suburban site ~10 km east of FSF), and to 8.5  $\mu\text{g m}^{-3}$  at SNFH (589 m above MSL, 33 km east of CLO). This reflects the influence of topography and the generally low vertical mixing potential due to weak boundary layer turbulence on many of the high PM<sub>2.5</sub> days. North of Fresno, the annual-average PM<sub>2.5</sub> concentration was relatively low even at the urban centers of Sacramento (S13, 11.1  $\mu\text{g m}^{-3}$ ) and San Francisco (SFA, 9.2  $\mu\text{g m}^{-3}$ ), with the highest annual-average concentration of 17.3  $\mu\text{g m}^{-3}$  observed at Modesto (M14).

[15] The stable atmosphere surrounding the Sierra Nevada and coastal mountains prevents precursor gases and PM released in the SJV from rapidly dispersing. To some extent, the valley is also isolated from the influences of outside sources. This is especially true for the southern SJV because the elevation of the valley floor generally increases from north to south as far as Fresno and descends south of Fresno. The five most northwestern sites in this network, located at Bodega Bay (BODG), BTI, SFA, S13, and Stockton (SOH), all have elevations less than 10 m above MSL. Marine air enters the SJV through the Carquinez Strait east of the San Francisco Bay area, leading to the lower PM<sub>2.5</sub> in the northern valley. The highest annual-average water-soluble sodium ( $\text{Na}^+$ ; a sea salt marker) concentrations were found at coastal sites west of the valley (BODG, SFA, and Livermore (LVR1)) where annual-average PM<sub>2.5</sub> and  $\text{Na}^+$  concentrations were 9.3 and 1.7, 9.2 and 0.58, and 10.6 and 0.32  $\mu\text{g m}^{-3}$ , respectively. Three sites in the northern valley, S13, BTI, and SOH, also experienced higher annual-average  $\text{Na}^+$  concentration (0.24–0.28  $\mu\text{g m}^{-3}$ ) than FSF (0.11  $\mu\text{g m}^{-3}$ ) and BAC (0.13  $\mu\text{g m}^{-3}$ ). The lower PM<sub>2.5</sub> concentrations at S13 and SOH compared with higher concentrations at down-valley urban sites demonstrate the influence of clean marine air in the northern valley.

[16] As shown in Figure 3, 24-hour PM<sub>2.5</sub> concentrations at FSF were low from mid-February 2000 to late October 2000, but frequently exceeded 15  $\mu\text{g m}^{-3}$  from November to January, and reached a maximum of 148  $\mu\text{g m}^{-3}$  on 1 January 2001. A similar temporal pattern was found at BAC, which often reported higher PM<sub>2.5</sub> concentrations than FSF. In addition to the increased RWC emissions during winter [Magliano *et al.*, 1999; Schauer and Cass, 2000], the meteorological effect (i.e., prolonged Great Basin highs causing subsidence) on the ventilation of pollutants and formation of secondary aerosol also contributes to the seasonal cycle. The regional transport ANGI site, located in the ancient Tulare Lake bed, surrounded by farm fields and sparse residences, experienced wintertime PM<sub>2.5</sub> concentrations similar to those at FSF and BAC. High winter concentrations at the other two interbasin anchor sites (BTI and SNFH) were much less pronounced. BODG in Figure 3 represents the northern boundary/background site

of the SJV, while the ACP (373 m above MSL) and TEH2 (1229 m above MSL) sites represent the eastern and southern intra and interbasin transport sites. No appreciable seasonal variations were observed at these boundary and transport sites, especially at BODG and TEH2; the background PM<sub>2.5</sub> level, which is often influenced by long-range (synoptic-scale) transport, appeared to be consistent year-round.

[17] The patterns of temporal variations in Figure 3 are consistent with limited differences in PM<sub>2.5</sub> spring (March to May) and summer (June to August) averages (Table 2). Urban-rural contrast in the northern SJV was minimal during spring and summer. For example, average spring PM<sub>2.5</sub> concentration at BODG (10.5  $\mu\text{g m}^{-3}$ ) compared well with those at FSF (11.2  $\mu\text{g m}^{-3}$ ) and the Fresno residential site (FRES; 9.0  $\mu\text{g m}^{-3}$ ). However, the source-dominated dairy site (FEDL) reported elevated average PM<sub>2.5</sub> concentrations (25–28  $\mu\text{g m}^{-3}$ ) during summer and fall, and reached a maximum of 39  $\mu\text{g m}^{-3}$  in winter.

[18] CRPAQS annual measurements may be divided into high ( $C_{\text{high}}$ ; 1 November 2000 to 31 January 2001) and low ( $C_{\text{low}}$ ; 1 February 2000 to 31 October 2000) PM<sub>2.5</sub> periods. As shown in Table 2, PM<sub>2.5</sub> approached 15  $\mu\text{g m}^{-3}$  at Bakersfield (BAC, EDI), even during the low period. The maximum  $C_{\text{low}}$  occurred at the source-dominated FEDL site (24  $\mu\text{g m}^{-3}$ ). The contributions of PM<sub>2.5</sub> during  $C_{\text{high}}$  to annual averages (i.e.,  $F_{\text{high}}$ , defined in Table 2), ranged from 13% at China Lake (CHL) to 72% at M14.  $C_{\text{high}}$  contributed more than 50% of annual-average PM<sub>2.5</sub> concentrations at most sites inside the valley, 55% at the BAC, and 63% at the FSF urban centers.  $F_{\text{high}}$  was <25% only at three sites in the network: CHL (10%), MOP (17%), and Olancho (OLW; 15%), all of which are located in the Mojave Desert or Great Basin Valleys. The slightly higher  $C_{\text{low}}$  than  $C_{\text{high}}$  at these desert sites is consistent with previously observed transport from the SJV and southern California during nonwinter months [Green *et al.*, 1992].

#### 4. PM<sub>2.5</sub> Chemical Composition

[19] Table 2 presents the annual-average concentrations of five main PM<sub>2.5</sub> components (i.e.,  $\text{NH}_4\text{NO}_3$ , ammonium sulfate [ $(\text{NH}_4)_2\text{SO}_4$ ], organic matter [OM = 1.4  $\times$  OC], EC, and crustal material), as well as the PM<sub>2.5</sub> mass balance. CRPAQS confirms previous studies conducted in the SJV [e.g., Chow *et al.*, 1992, 1993a, 1996, 1999] that PM<sub>2.5</sub> consists mainly of  $\text{NH}_4\text{NO}_3$  and carbonaceous material. Volatilized  $\text{NH}_4\text{NO}_3$  from the backup filter is not included in the reconstructed mass (defined in Table 2) since PM<sub>2.5</sub> mass determined from Teflon-membrane filters does not contain volatilized  $\text{NO}_3^-$  [Chow *et al.*, 2005b]. The OC multiplier of 1.4, which accounts for unmeasured hydrogen, oxygen, and other elements in OM, was derived from the analysis of organic compounds in urban aerosols [Grosjean and Friedlander, 1975; White and Roberts, 1977]. This factor is environment-specific with lower values found in urban or source-dominated atmospheres, and with higher values in remote locations [Turpin and Lim, 2001; El-Zanan *et al.*, 2005]. A value of 1.4, however, remains useful for cross-environment averages [Russell, 2003]. Because the CRPAQS network contained both urban and rural

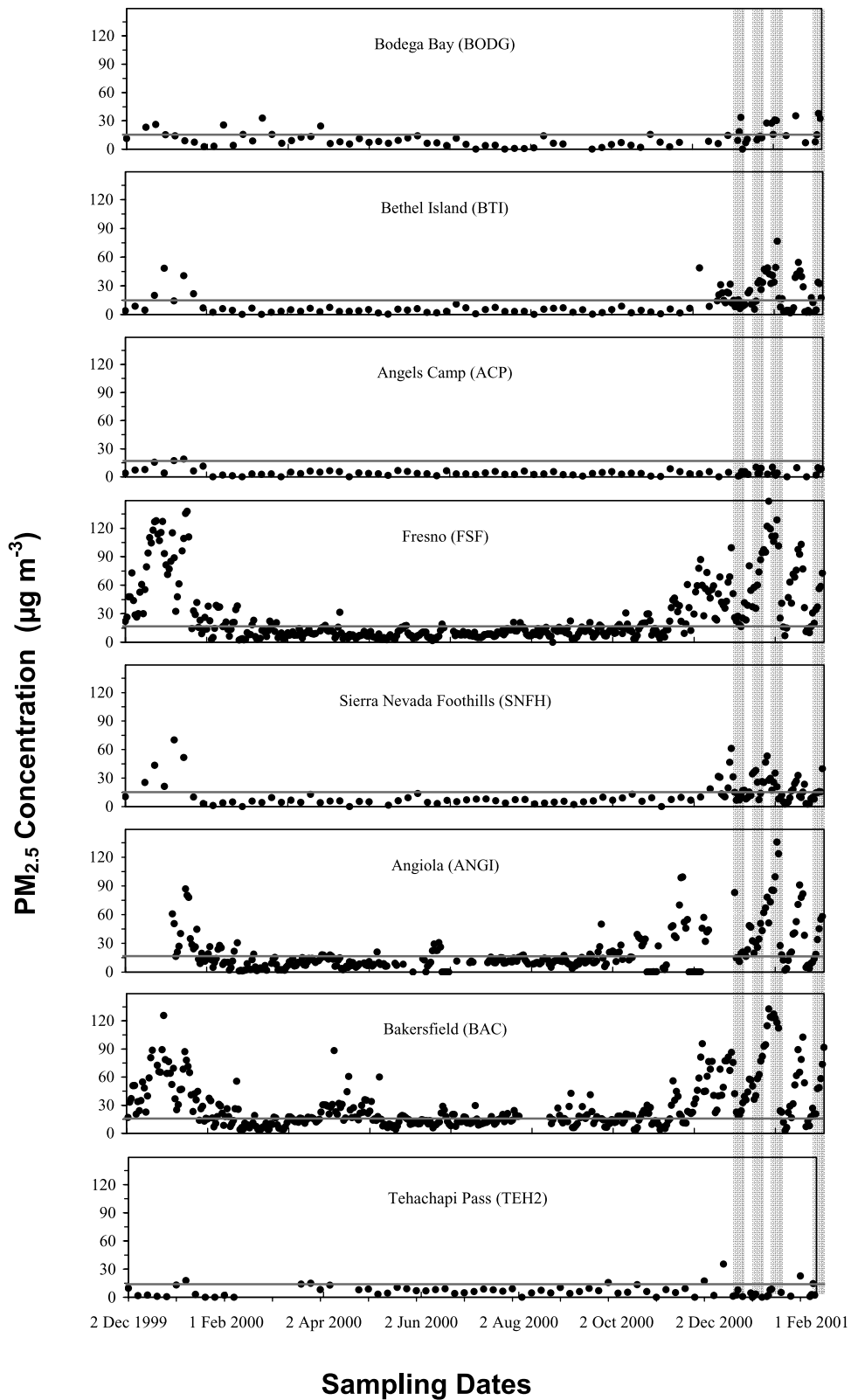


**Figure 3.** Time series of 24-hour average PM<sub>2.5</sub> concentration at selected sites during CRPAQS including northern boundary/background site (BODG); interbasin anchor sites (BTI, SNFH); eastern transport site (ACP); southern transport site (TEH2); regional transport anchor site (ANGI); and urban anchor sites (FSF and BAC). The Y axis is PM<sub>2.5</sub> concentration ( $\mu\text{g m}^{-3}$ ). Vertical shaded areas indicate the Winter Intensive Operating Periods (IOPs).

sites, the value of 1.4 is appropriate. This factor has also been adopted for mass- and light-extinction reconstruction in the IMPROVE network of U.S. national parks and wilderness areas [Malm *et al.*, 1994].

[20] Besides the factors applied to OC and mineral oxides, potential biases in mass closure include sampling artifacts caused by volatile organic compounds (VOCs). Adsorption of VOCs onto quartz-fiber filters [Turpin *et al.*, 1994; Chow and Watson, 2002; Chow *et al.*, 2006b] is known to bias OM mass positively. This artifact may be partially compensated for by the evaporation of OM from the filters [Zhang and McMurry, 1987; Chen *et al.*, 2002; Subramanian *et al.*, 2004]. The relative importance of positive and negative sampling biases was examined at FSF using parallel denuded (organic vapor denuder) and nondenuded channels followed by quartz-fiber/quartz-fiber filter packs [Watson and Chow, 2002b; Chow *et al.*, 2006b]. Average nondenuded and denuded front quartz-fiber filter OC concentrations were  $11.8 \pm 1.2$  and  $10.8 \pm 1.1 \mu\text{g m}^{-3}$ , respectively, during winter; and  $4.8 \pm 0.6$  and  $3.9 \pm 0.5 \mu\text{g m}^{-3}$ , respectively, during summer. Average nondenuded and denuded backup quartz-fiber filter OC concentrations were  $2.1 \pm 0.3$  and  $0.25 \pm 0.41 \mu\text{g m}^{-3}$ , respectively, during winter; and  $1.84 \pm 0.28$  and  $0.50 \pm 0.42 \mu\text{g m}^{-3}$ , respectively, during summer. On the basis of the nondenuded backup quartz-fiber filter concentrations, a seasonally constant sampling artifact of  $\sim 3 \mu\text{g m}^{-3}$  OM could bias the mass closure for samples with low concentrations. The four lowest ( $< 5 \mu\text{g m}^{-3}$ ) annual-average PM<sub>2.5</sub> concentrations in Table 2 (i.e., CHL, OLW, ACP, and MOP) have mass closure  $> 200\%$ . In these cases, the positive VOC artifact appeared to dominate, which is consistent with other recent studies [e.g., Subramanian *et al.*, 2004; Chow *et al.*, 2006b].

[21] PM<sub>2.5</sub> mass closure was  $< 100\%$  at FSF, FEDL, and BRES, where PM<sub>2.5</sub> concentrations were relatively high. This may be due in part to water retention by hygroscopic species, such as NH<sub>4</sub>NO<sub>3</sub> and (NH<sub>4</sub>)<sub>2</sub>SO<sub>4</sub>, and/or an underestimation of the OC multiplier [Andrews *et al.*, 2000; Turpin and Lim, 2001; Rees *et al.*, 2004; El-Zanan *et al.*, 2005; Khlystov *et al.*, 2005]. Nevertheless, measured and reconstructed mass were highly correlated, with an R<sup>2</sup> of 0.94. NH<sub>4</sub>NO<sub>3</sub> and OM are the most dominant components of PM<sub>2.5</sub>, accounting for 66% and 73% of PM<sub>2.5</sub> mass at urban FSF and BAC, respectively.

[22] A triangle-based cubic interpolation algorithm [Sandwell, 1987; Barber *et al.*, 1996] was used to visualize the spatial variability. Sites with more than 30% missing data (see Table 2) were excluded from the analysis. Average concentrations of PM<sub>2.5</sub> mass and its chemical components during C<sub>low</sub> and C<sub>high</sub> periods are compared along three geographic cross sections in Figure 4 (A, B, and C, defined in Figure 2a). These cross sections all intersect at FSF and cover major SJV geographical features. During the C<sub>low</sub> period, urban sites experienced PM<sub>2.5</sub> concentrations slightly higher than rural sites. A nearly uniform OM distribution was observed along cross section C that stretches between the Sierra Nevada and the coastal mountains (119.3–120.5° W longitude). Average OM concentrations at Helm (HELM), FSF, and SNFH during the C<sub>low</sub> period were 5.3, 6.8, and 6.4  $\mu\text{g m}^{-3}$ , respectively. EC, which is not subject to sampling artifacts, showed a similar pattern, averaging 1.4, 1.1, and 1.2  $\mu\text{g m}^{-3}$ , respectively.

Within the SJV, pNH<sub>4</sub>NO<sub>3</sub> was generally  $< 7 \mu\text{g m}^{-3}$ , decreasing to  $\sim 2 \mu\text{g m}^{-3}$  at the elevated mountain sites of ACP, SNFH, and CHL. Most ( $> 80\%$ ) of the pNH<sub>4</sub>NO<sub>3</sub> was found on the front filter, except at BAC (cross section B) where more than 50% was found on the backup filter. (NH<sub>4</sub>)<sub>2</sub>SO<sub>4</sub> and crustal material were minor components of PM<sub>2.5</sub>.

[23] The pNH<sub>4</sub>NO<sub>3</sub> in the southern SJV was much higher during the C<sub>high</sub> period than the C<sub>low</sub>, with the highest average concentration of  $\sim 30 \mu\text{g m}^{-3}$  observed at BAC. Elevated pNH<sub>4</sub>NO<sub>3</sub> concentrations were not limited to urban areas. The rural HELM site in central Fresno County (55 m above MSL in cross section C),  $\sim 41$  km to the west of FSF, reported a pNH<sub>4</sub>NO<sub>3</sub> concentration of  $\sim 17.1 \mu\text{g m}^{-3}$ , close to levels found in the Fresno area (19–22  $\mu\text{g m}^{-3}$ ). The pNH<sub>4</sub>NO<sub>3</sub> average was even higher at ANGI, approaching 22  $\mu\text{g m}^{-3}$ . However, pNH<sub>4</sub>NO<sub>3</sub> concentrations decreased rapidly with site elevation and location outside the SJV. The MOP site (832 m above MSL in the Mojave Desert) reported 1.1 and 1.3  $\mu\text{g m}^{-3}$  pNH<sub>4</sub>NO<sub>3</sub> during the C<sub>low</sub> and C<sub>high</sub> periods, respectively. Figure 4 demonstrates that widespread pNH<sub>4</sub>NO<sub>3</sub> is the major contributor to wintertime basin-wide PM<sub>2.5</sub> episodes.

[24] NO<sub>x</sub> is converted to HNO<sub>3</sub> by photochemical processes that also involve VOCs [Stockwell *et al.*, 2000; Pun and Seigneur, 2001]. HNO<sub>3</sub> reacts reversibly with NH<sub>3</sub> to form solid NH<sub>4</sub>NO<sub>3</sub>. If the RH is high enough, the solid deliquesces to form ions in solution. Winter's cold and humid weather favors NH<sub>4</sub>NO<sub>3</sub> over gaseous NH<sub>3</sub> and HNO<sub>3</sub> [Seinfeld and Pandis, 1998; Moya *et al.*, 2001; Takahama *et al.*, 2004]. The seasonal cycle of the NH<sub>3(g)</sub>/NH<sub>4(p)</sub> ratio at FSF (Figure 5) confirms the shift of this equilibrium toward NH<sub>3</sub> in the spring-fall period. Surface wind speeds in the SJV are often  $< 1 \text{ m s}^{-1}$  during winter, with variable wind directions. Surface transport distances estimated from these wind speeds are insufficient to account for the mixing of nonurban NH<sub>3</sub> emissions with urban NO<sub>x</sub> and VOC emissions for the formation of widespread NH<sub>4</sub>NO<sub>3</sub> [Smith and Lehrman, 1994]. The spatial distribution of NH<sub>4</sub>NO<sub>3</sub> corroborates the hypothesis of Watson and Chow [2002a] that transport/mixing is facilitated by a valley-wide mixed layer above the shallow ( $\sim 20$  m) nighttime surface layer.

[25] In contrast with pNH<sub>4</sub>NO<sub>3</sub>, no appreciable increases of EC or OM were detected at rural sites, such as BTI, HELM, and ANGI (Figure 4) during the C<sub>high</sub> period. While pNH<sub>4</sub>NO<sub>3</sub> increased from 3.5  $\mu\text{g m}^{-3}$  (C<sub>low</sub>) to 17.1  $\mu\text{g m}^{-3}$  (C<sub>high</sub>) at HELM, the EC concentration remained between 1.4 and 1.7  $\mu\text{g m}^{-3}$ . This is consistent with a weak source of primary PM emissions in the rural areas. EC concentrations of 4  $\mu\text{g m}^{-3}$  or higher were found at the urban sites M14, S13, FSF, and BAC. OM generally tracked with EC, which exacerbated urban PM pollution already enhanced by NH<sub>4</sub>NO<sub>3</sub>. PM<sub>2.5</sub> water-soluble potassium (K<sup>+</sup>), a prominent marker for RWC emissions [Chow *et al.*, 1992], averaged 0.05 and 0.31  $\mu\text{g m}^{-3}$  during the C<sub>low</sub> and C<sub>high</sub> periods, respectively, at the FRES site. At BAC, K<sup>+</sup> concentrations were 0.07 and 0.34  $\mu\text{g m}^{-3}$  during the C<sub>low</sub> and C<sub>high</sub> periods, respectively, while the corresponding average ratios of soluble to total K were 0.37 and 0.87, respectively. It is evident that RWC caused elevated winter EC and OM concentrations in the urban areas.

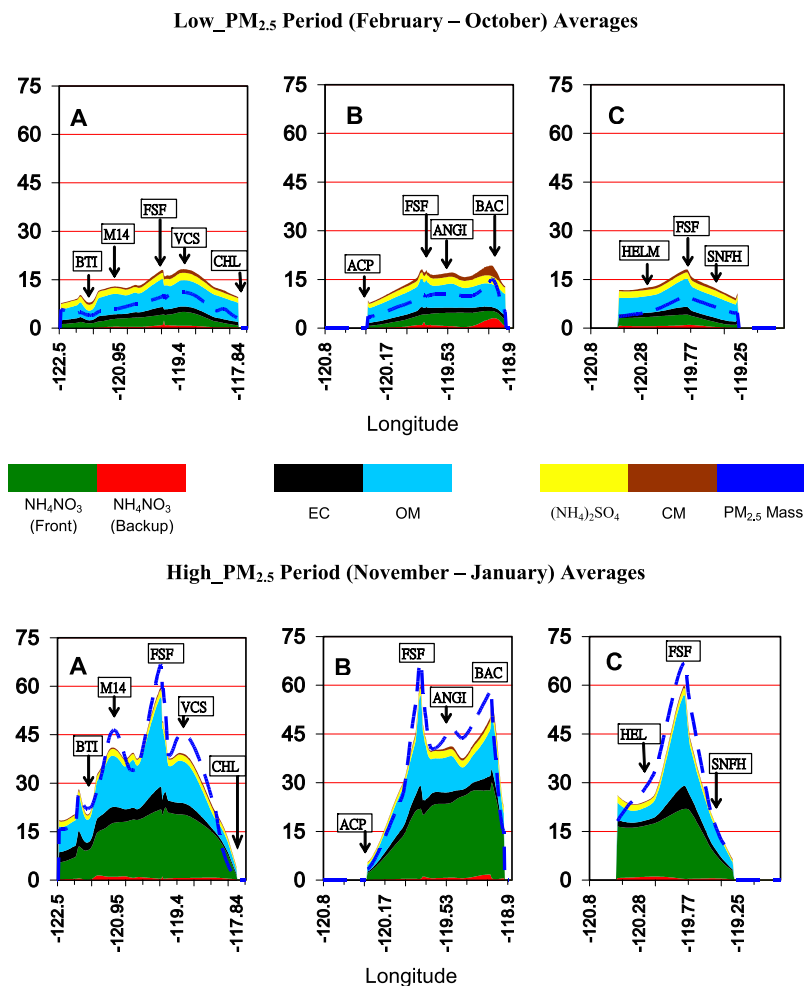


**Figure 4.** Chemical composition and mass closure of PM<sub>2.5</sub> along the geographical cross sections A, B, and C (defined in Figure 2a) for the low ( $C_{low}$ ) and high ( $C_{high}$ ) PM<sub>2.5</sub> periods during CRPAQS. The Y axes represent concentration ( $\mu\text{g m}^{-3}$ ). Sampling sites located approximately on each cross section are noted. The dashed line represents measured PM<sub>2.5</sub> mass.

[26] Levoglucosan is also a marker for RWC emissions [Simoneit *et al.*, 1999; Fine *et al.*, 2002; Simoneit, 2002; Mochida and Kawamura, 2004]. Rinehart *et al.* [2006] measured annual-average organic compound concentrations at 20 satellite sites in the SJV and reported high concentrations of levoglucosan at FSF. Poore [2002] showed that levoglucosan concentrations at FSF were five times higher during winter than summer.

[27] The summed concentrations of nonvolatilized  $\text{NH}_4\text{NO}_3$ , OM, and EC exceeded measured PM<sub>2.5</sub> mass during the  $C_{low}$  period (Figure 4). As discussed above, VOC adsorption on the front quartz-fiber filter is likely the major cause of mass closure  $>100\%$  during  $C_{low}$ . During  $C_{high}$ , the sum of chemical components did not explain PM<sub>2.5</sub> mass at the urban sites (Figure 4). The amount of water retained by  $\text{NH}_4\text{NO}_3$  on the Teflon-membrane filter (e.g., during weighing at  $35 \pm 5\%$  RH) is not expected to be a substantial fraction of the PM<sub>2.5</sub> concentration [Chan *et al.*, 1992]. The VOC adsorption artifact appeared to be temporally uniform regardless of the PM<sub>2.5</sub> concentration, as suggested by Chow *et al.* [2006b]. This implies that the artifact is more important for samples with PM<sub>2.5</sub>  $<15 \mu\text{g m}^{-3}$ . Note that 84% of the samples with PM<sub>2.5</sub> concentration  $>20 \mu\text{g m}^{-3}$

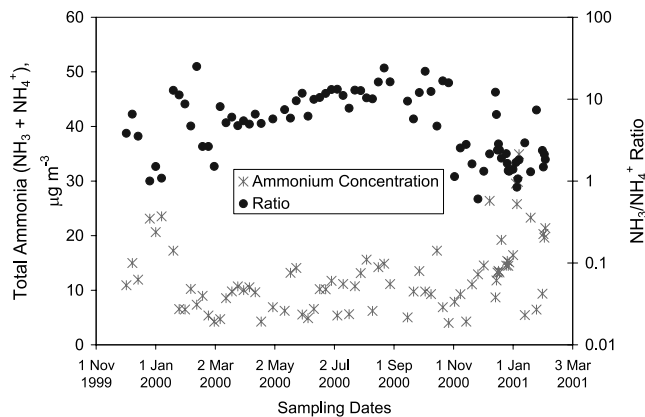


**Figure 5.** Seasonal variation of total ammonia ( $\text{NH}_3 + \text{NH}_4^+$  as  $\text{NH}_3$  equivalent) concentration and  $\text{NH}_3/\text{NH}_4^+$  ratio at the Fresno site (FSF) during CRPAQS. Note that the Y axis on the right has a logarithmic scale.

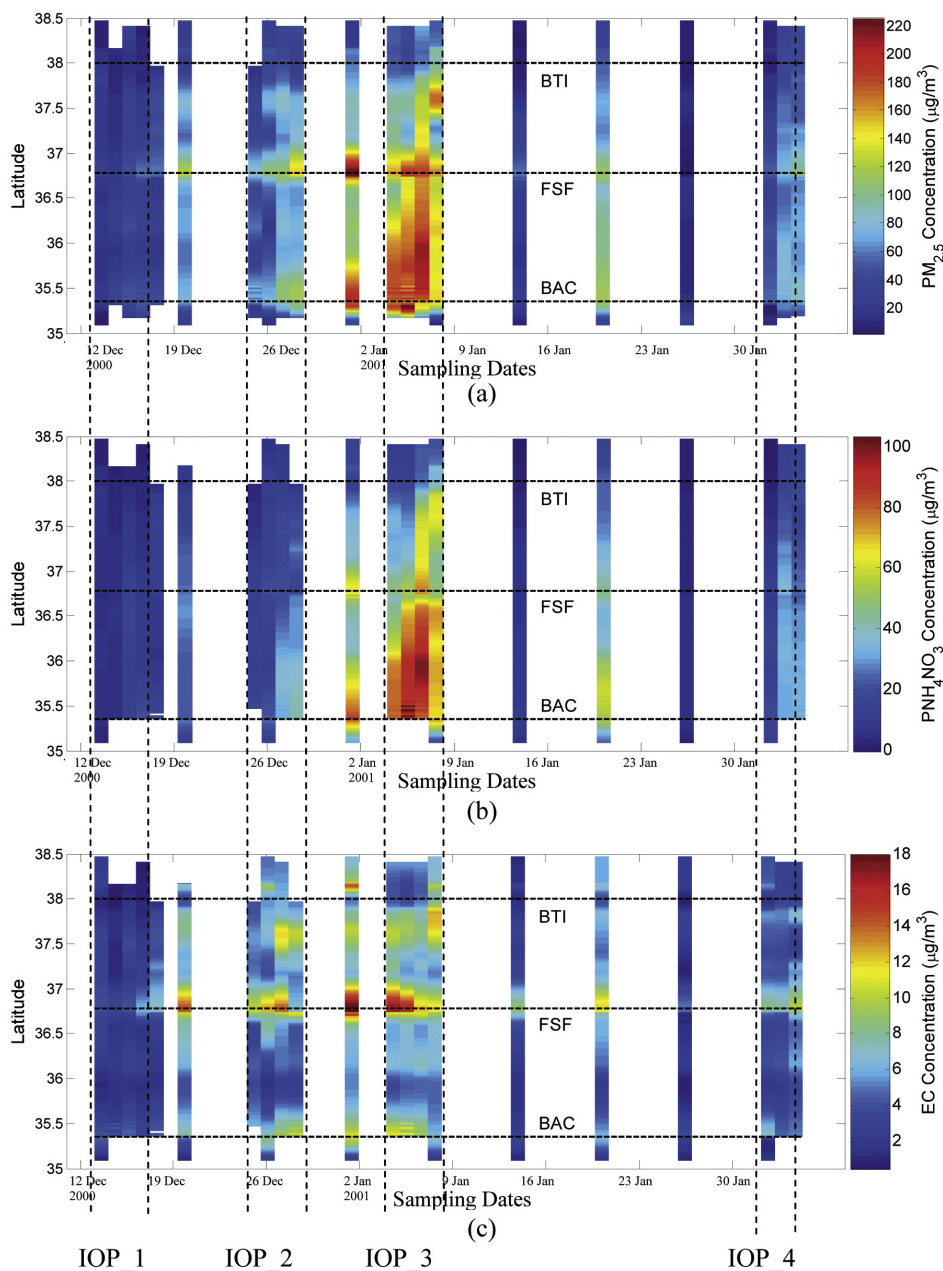


**Figure 6.** Spatial and temporal variations of (a) PM<sub>2.5</sub> mass, (b) particulate ammonium nitrate (pNH<sub>4</sub>NO<sub>3</sub>), and (c) elemental carbon (EC) across the four CRPAQS winter intensive operating periods (IOPs). The concentrations are those along the cross section D defined in Figure 2b (essentially a combination of the top portion of cross section A and bottom portion of B, shown in Figure 2a), calculated with a cubic-spline algorithm using all available measurements. Horizontal dashed lines indicate the latitude of Bethel Island (BTI), Fresno (FSF), and Bakersfield (BAC) sites.

showed mass closure at <110% regardless of the site; well within the  $\pm 10\%$  measurement uncertainties of the PM<sub>2.5</sub> mass.

## 5. Winter PM<sub>2.5</sub> Episodes

[28] The winter IOPs were selected from boundary layer stability forecasts, which were based on meteorological characteristics in the SJV (mixing height, wind speed, and RH) normally associated with high PM<sub>2.5</sub> concentrations. The selected four IOP periods are listed in Table 1. Five

time-integrated measurements (0000–0500, 0500–1000, 1000–1300, 1300–1600, and 1600–2400 LT) were taken during each IOP day. Daily PM<sub>2.5</sub> mass and chemical concentrations were calculated as time-weighted averages of the concentrations during these periods.

[29] Figure 6 presents the concentrations of PM<sub>2.5</sub> mass, pNH<sub>4</sub>NO<sub>3</sub>, and EC along geographic cross section D (defined in Figure 2b), which represents the valley's primary axis. No apparent contrasts for PM<sub>2.5</sub>, or its chemical components, were found during IOP<sub>1</sub> (15–18 December 2000). The pNH<sub>4</sub>NO<sub>3</sub> started accumulating during IOP<sub>2</sub>

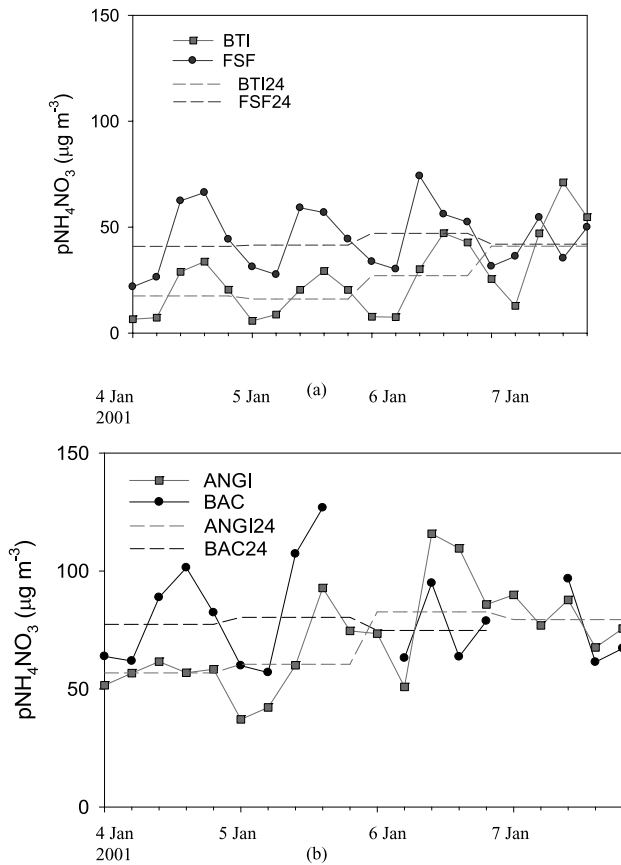


**Figure 7.** Diurnal and 24-hour average total particulate ammonium nitrate ( $pNH_4NO_3$ ) concentrations at (a) FSF and BTI and (b) ANGI and BAC during the 4–7 January 2001 IOP. Twenty-four-hour average concentrations are indicated by the dashed lines.

(26 December 2000) in the southern SJV and appeared to persist through early January 2001. High EC ( $>10 \mu g m^{-3}$ ) was also observed around urban centers such as M14, FSF, and BAC.

[30] A major PM<sub>2.5</sub> episode driven by  $pNH_3NO_3$  occurred during IOP\_3 (4–7 January 2001). From IOP\_2 through IOP\_3, the SJV was situated between a persistent high-pressure ridge over the Great Basin and a surface low off the southern California coast. On 4 January 2001,  $pNH_3NO_3$  in the southern SJV was  $75 \mu g m^{-3}$ , and by 5 January 2001, this plume blanketed a broad region between BAC and FSF. The highest 24-hour average  $pNH_4NO_3$  concentration of this episode ( $83 \mu g m^{-3}$ ) was measured at ANGI on 6 January 2001. For the first time during winter, M14 recorded a  $pNH_4NO_3$  concentration approaching  $60 \mu g m^{-3}$  (6–7 January 2001). While  $pNH_4NO_3$  gradually dissipated in the southern SJV after 6 January 2001, the northern boundary BTI site reported a  $pNH_4NO_3$  concentration of  $40 \mu g m^{-3}$  on 7 January 2001 compared with  $\sim 50 \mu g m^{-3}$  at FSF. The  $pNH_4NO_3$  peak moved northward, consistent with the influence of regional transport.

[31] This episode is examined in greater detail in Figure 7 with subdaily  $pNH_4NO_3$  concentrations at northern (FSF and BTI) and southern (BAC and ANGI) urban-rural pairs. All four sites showed a clear diurnal pattern with a midday peak caused by photochemical production and turbulent mixing, as suggested by *Watson and Chow* [2002a]. While there was virtually no increase in the 24-hour average  $pNH_4NO_3$  concentration at either urban site, it increased throughout the IOP at both rural sites; occurring at ANGI on 6 January 2001 and at BTI on 6–7 January 2001. This again supports the conceptual model that urban precursors are transported aloft to rural locations, where they mix with nonurban  $NH_3$  emissions.

[32] Figure 8 presents the upper air wind structure measured with a wind profiler at ANGI. Wind speeds generally increased with altitude, and a sharp reversal of wind direction was observed during the evening of 5 January 2001 that explains the northward transport on 6–7 January 2001.

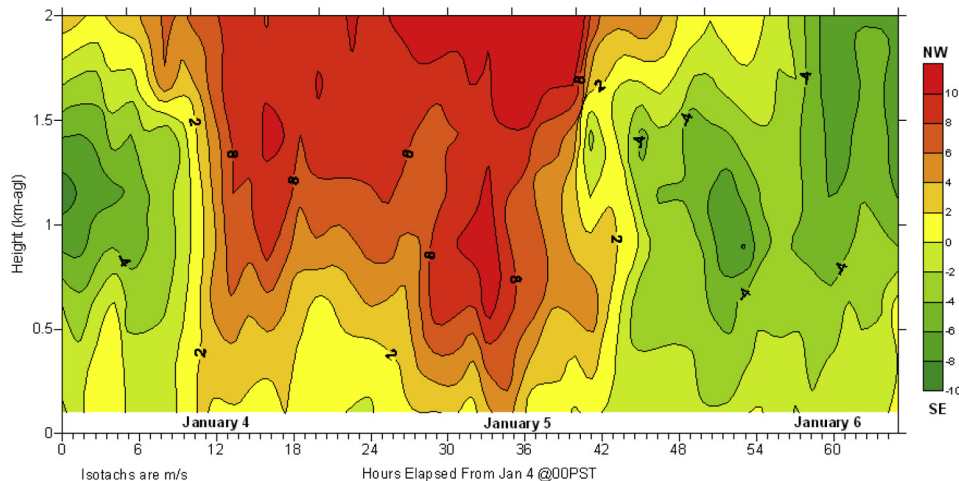


**Figure 8.** Wind speed from the northeast to southwest as a function of altitude measured at the Angiola (ANGI) site during IOP\_3, 4–6 January 2001. Positive component is flow from northwest to southeast.

**Table 3.** Twenty-Four-Hour Average Concentrations ( $\mu\text{g m}^{-3}$ ) at FSF and BAC During IOP3

Site	Date	OM <sup>a</sup>	EC <sup>b</sup>	K <sup>+c</sup>	NH <sub>3</sub> <sup>d</sup>	TNH <sub>3</sub> <sup>e</sup>	pNH <sub>4</sub> NO <sub>3</sub> <sup>f</sup>	NO <sub>x</sub> <sup>g</sup> ppb	O <sub>3</sub> <sup>h</sup> ppb	T <sub>i</sub> <sup>i</sup> °C	RH <sub>i</sub> <sup>j</sup> %
FSF	4 Jan. 2001	39	10.3	0.52	16	25	41	171	8.2	7.2	71
BAC	4 Jan. 2001	32	8.5	0.56	26	42	77	200	12.7	7.3	74
FSF	5 Jan. 2001	42	9.7	0.57	15	24	42	165	10.8	6.8	69
BAC	5 Jan. 2001	29	6.4	0.66	16	34	80	171	8.4	6.7	80
FSF	6 Jan. 2001	52	10.3	0.62	16	26	47	124	15.9	7.7	64
BAC	6 Jan. 2001	31	6.7	0.59	22	38	75	138	12.8	9.5	67
FSF	7 Jan. 2001	38	8.2	0.54	21	30	42	85	14.4	9.3	52
BAC	7 Jan. 2001	22	5.5	0.43	21	37	72	93	13.9	9.5	62

<sup>a</sup>Organic matter (OC  $\times$  1.4).

<sup>b</sup>Elemental carbon.

<sup>c</sup>Water-soluble potassium ion.

<sup>d</sup>Gaseous ammonia.

<sup>e</sup>Ammonia plus ammonium as ammonia equivalent.

<sup>f</sup>Total particulate ammonium nitrate (NH<sub>4</sub>NO<sub>3</sub>) = 1.29  $\times$  pNO<sub>3</sub><sup>-</sup> (the sum of front-filter nonvolatilized nitrate [NO<sub>3</sub><sup>-</sup>] plus backup filter volatilized NO<sub>3</sub><sup>-</sup>).

<sup>g</sup>Nitrogen oxides.

<sup>h</sup>Ozone.

<sup>i</sup>Temperature.

<sup>j</sup>Relative humidity.

[33] Twenty-four-hour average NO<sub>x</sub> and ozone (O<sub>3</sub>) concentrations, as well as temperature (T) and RH, at FSF and BAC during IOP\_3 are compared with corresponding gas and PM concentrations in Table 3. The major difference between the two urban sites is higher pNH<sub>4</sub>NO<sub>3</sub> concentrations at BAC, which is consistent with higher NO<sub>x</sub> and total ammonia (TNH<sub>3</sub> = NH<sub>3</sub> plus NH<sub>4</sub><sup>+</sup> as NH<sub>3</sub> equivalent) at BAC. Low surface wind speeds minimize dispersion of primary PM<sub>2.5</sub> components near their sources. Primary PM<sub>2.5</sub> includes EC and OM from RWC, vehicle exhaust, and crustal material from resuspended dust. IOPs\_2 and\_3 experienced mean surface wind speeds of 0–2 m s<sup>-1</sup> at FSF and a substantial accumulation of EC, especially on 1, 4, and 5 January 2001 (Figure 6). High EC concentrations also occurred at M14 and BAC. Soluble K<sup>+</sup> concentrations were similar at FSF and BAC (Table 3). While EC and OM concentrations were about 50% higher at FSF, the EC/OM ratios at both FSF and BAC sites were nearly identical (0.23  $\pm$  0.03 and 0.24  $\pm$  0.02, respectively). By 8 January 2001, the surface low had advanced eastward, resulting in precipitation on 9 January 2001 that ended the episode. Both EC and pNH<sub>4</sub>NO<sub>3</sub> concentrations decreased to less than 10  $\mu\text{g m}^{-3}$  by 13 January 2001 at FSF and BAC.

[34] Similar synoptic meteorology and PM<sub>2.5</sub> spatial distribution patterns were observed during IOP\_2 and IOP\_4. Valley-wide exceedances of 65  $\mu\text{g m}^{-3}$  (the value for the 98th percentile averaged over three years for the 24-hour PM<sub>2.5</sub> NAAQS) were found at 26 sites during IOPs\_2, 3, and 4. In rural areas, these high concentrations consisted mainly of pNH<sub>4</sub>NO<sub>3</sub>, while urban PM<sub>2.5</sub> contained larger carbonaceous fractions.

## 6. Zones of Representation

[35] In designing an ambient air quality monitoring network, it is essential to know the extent to which community exposure monitoring sites represent their surroundings. The CRPAQS network included sites representing regional- (100–1000 km) (U.S. EPA, 1997), urban- (4–100 km), neighborhood- (0.5–4 km), middle- (0.1–0.5 km), and micro- (0.01 km–0.1 km) scales. The median distance between two neighboring sites in the CRPAQS network

was  $\sim$ 25 km, but some sites were located less than 1 km apart in order to contrast and compare different micro-environments [Watson and Chow, 2002a]. For example, a roadside site (FREM) and a residential site (FRES) were located  $\sim$ 1 km west and  $\sim$ 0.5 km east of the FSF.

[36] Most previous studies of community exposure consisted of two or three sites, typically locating one in the city center, and others in surrounding neighborhoods [e.g., Louie *et al.*, 2005; Chow *et al.*, 2006c]. In contrast, the CRPAQS network covered a much larger area containing many more urban and rural sites. The zones of representation can therefore be quantified by spatial interpolation of measured concentrations through the use of contour plots. This interpolation relies on the assumption of a smooth transition between each pair of neighboring sites. The validity of this hypothesis improves as the number (or density) of monitoring sites increases, because finer features of the spatial variability will be captured.

[37] The first step was to estimate concentration fields and to map the concentration gradients (e.g., Figure 2a). The zone of representation is defined as the radius of a circular area in which a species concentration varies by no more than  $\pm$ 20% as it extends outward from the center monitoring site. The criterion of 20% is chosen since it translates to  $\sim$ 10% or less of the difference between the center site concentration and the average over the entire circular area, where 10% is on the order of the measurement uncertainty. The approach provides a quantitative comparison of spatial distributions between different species, seasons, and sites. Uncertainties resulting from inadequate spatial resolution may be mitigated by appropriate site selection based on county-level emission inventories [e.g., California Air Resources Board, 2004]. Since increasing the number of sites would likely reduce the zone coverage, this current approach gives the upper limit of the “true” zone sizes.

[38] Table 4 summarizes the zones of representation of 11 community exposure sites and two interbasin transport sites (BTI and ANGI) for annual, seasonal, and IOP periods. FSF represents different zones for annual pNH<sub>4</sub>NO<sub>3</sub> (19 km) and EC (<1 km), consistent with the sources and meteorology at FSF. The major contrast among the three sampling sites in Fresno (FSF, FRES, FREM) and its suburban site (CLO,

**Table 4.** Zone of Representation for Eleven Community Exposure and Two Interbasin Transport Sites in the San Joaquin Valley on Different Temporal Scales<sup>a</sup>

Site Code <sup>b</sup>	Annual: Zone of Representation, km			C <sub>high</sub> : High_PM <sub>2.5</sub> (Nov. to Jan.): Zone of Representation, km			C <sub>low</sub> : Low_PM <sub>2.5</sub> (Feb. to Oct.): Zone of Representation, km			Episode (7 Jan. 2001): Zone of Representation, km		
	PM <sub>2.5</sub>	pNH <sub>4</sub> NO <sub>3</sub>	EC	PM <sub>2.5</sub>	pNH <sub>4</sub> NO <sub>3</sub>	EC	PM <sub>2.5</sub>	pNH <sub>4</sub> NO <sub>3</sub>	EC	PM <sub>2.5</sub>	pNH <sub>4</sub> NO <sub>3</sub>	EC
S13	12	12	12	10	11	11	54	31	37	6	10	15
<b>BTI</b>	<b>15</b>	<b>13</b>	<b>10</b>	<b>14</b>	<b>10</b>	<b>9</b>	<b>15</b>	<b>16</b>	<b>10</b>	<b>5</b>	<b>10</b>	<b>9</b>
M14	22	20	23	19	20	17	25	20	34	6	18	12
MRM	19	14	14	15	14	13	27	15	14	1	12	11
CLO	6	10	3	6	10	3	9	11	3	5	4	4
<b>FSF</b>	<b>11</b>	<b>19</b>	<1	<b>10</b>	<b>18</b>	<1	<b>13</b>	<b>12</b>	<b>1</b>	<b>11</b>	<b>2</b>	<b>8</b>
SELM	13	21	9	12	19	8	20	23	12	1	10	12
VCS	23	19	28	21	18	23	28	21	30	14	9	16
COP	22	23	6	21	27	6	16	16	6	5	18	6
<b>ANGI</b>	<b>19</b>	<b>19</b>	<b>4</b>	<b>19</b>	<b>19</b>	<b>4</b>	<b>16</b>	<b>16</b>	<b>3</b>	<b>12</b>	<b>14</b>	<b>4</b>
OLD	6	21	4	15	12	3	3	5	7	8	14	3
<b>BAC</b>	<b>7</b>	<b>12</b>	<b>1</b>	<b>4</b>	<b>3</b>	<b>2</b>	<b>5</b>	<b>8</b>	<b>6</b>	<b>6</b>	<b>5</b>	<b>4</b>
MOP	8	3	20	3	1	7	15	8	55	14	1	10

<sup>a</sup>Sites are arranged from north to south; anchor sites are noted in bold.

<sup>b</sup>See Table 1 for site description.

7 km east) is due to carbonaceous material, probably from mobile sources, rather than pNH<sub>4</sub>NO<sub>3</sub>. Neighborhood-scale monitoring is needed to resolve the spatial variability of EC, and perhaps OM, in this urban area. Because it is located in downtown Bakersfield, the BAC site also has a small zone of representation for EC (~1 km). The difference between BAC and its satellite site (BRES, 2 km west) is ~40%. BTI is influenced by nearby cities, including San Francisco (SFA, 70 km west), Sacramento (S13, 50 km northeast), and Stockton (SOH, 30 km east). It represents a consistent zone (10–15 km) for PM<sub>2.5</sub> mass, pNH<sub>4</sub>NO<sub>3</sub>, and EC. In general, the zone size for pNH<sub>4</sub>NO<sub>3</sub> is more consistent than for EC across different sites. For annual PM<sub>2.5</sub>, BTI and ANGI represent areas with radii of 15 and 19 km, respectively, larger than the urban sites of FSF and BAC (7–11 km).

[39] The zones of representation during the C<sub>high</sub> period were similar to those of the annual-average zones except at BAC, where the zone for pNH<sub>4</sub>NO<sub>3</sub> was much smaller (3 km). Such a small zone reflects the facts that BAC is located at the southern boundary of the NH<sub>4</sub>NO<sub>3</sub> plume and that NH<sub>4</sub>NO<sub>3</sub> concentration decreases sharply to the south. This also explains the small zone of representation of MOP, which is an elevated site south of BAC. For the C<sub>low</sub> period, the zone of representation of EC at MOP was close to the background level in neighboring rural areas and this site represented a zone with a radius of up to 55 km. Larger EC zones were also found at other community exposure sites during the C<sub>low</sub> period; for example, VCS (30 km), M14 (34 km), and S13 (37 km). To some extent, this reflects less urban-rural contrast in summer with regard to EC concentration. Sharp gradients in EC concentration near rural ANGI and COP, however, warrant further investigation.

[40] The pNH<sub>4</sub>NO<sub>3</sub> zone appeared to be consistent between the C<sub>low</sub> and C<sub>high</sub> periods for most of the sites in the valley (Table 4). Pollutants exhibit more spatial inhomogeneity for a shorter averaging period, as expected.

[41] Factors affecting the zone size are complex. Rural sites do not necessarily have larger zones of representation than urban sites, because many of the rural sites in the SJV are close to the valley boundary, or located between two

urban centers where concentration gradients are steep. Future ambient network design efforts should consider findings from this study to determine more optimal site location and density. For instance, more sites could be located near ANGI and COP (mainly to the west) to verify a consistently high EC gradient. Temporary satellite sites equipped with portable monitors are a cost effective means of acquiring this information.

## 7. Discussion and Conclusions

[42] CRPAQS shows that PM<sub>2.5</sub> mass and NH<sub>4</sub>NO<sub>3</sub> concentrations vary as a function of elevation, and suggests that vertical mixing is limited in the SJV to about 600 m above MSL. While widespread PM<sub>2.5</sub> exceedances (up to 30 μg m<sup>-3</sup>) occurred in the southern SJV, PM<sub>2.5</sub> concentration was at near-background levels toward the mountainous boundary.

[43] For most of the sites within the SJV, 50–75% of annual-average PM<sub>2.5</sub> concentrations occurred from November to January. Elevated PM<sub>2.5</sub> at nonurban sites was caused by high concentrations of NH<sub>4</sub>NO<sub>3</sub>. During winter, temperature, RH, and the stable valley boundary layer were favorable for the formation of NH<sub>4</sub>NO<sub>3</sub> from its NH<sub>3</sub> and HNO<sub>3</sub> precursors. High EC and OM levels exacerbate air quality most severely at urban sites. This is consistent with the use of wood fuel for home heating in winter, as well as motor vehicle emissions. PM<sub>2.5</sub> mass closure was typically >100% for samples with concentrations <15 μg m<sup>-3</sup>, likely reflecting a positive VOC sampling artifact on quartz-fiber filters. For samples with PM<sub>2.5</sub> >20 μg m<sup>-3</sup>, however, this artifact was relatively less significant and the mass closure was close to, or less than, 100%.

[44] Lateral dispersion of the pollution plume became evident during winter episodes, an observation that supports the hypothesis of the role of upper layer currents on the valley-wide formation and transport of NH<sub>4</sub>NO<sub>3</sub>. Gradients of spatially interpolated concentrations show that most sites in the network appeared to represent zone sizes on an urban scale (4–100 km) or a neighborhood scale (0.5–4 km). In general, the annual NH<sub>4</sub>NO<sub>3</sub> zone sizes across different sites

were not the same as those for EC, consistent with a more inhomogeneous EC distribution in the valley. This information can be used to refine long-term monitoring networks in the future.

[45] **Acknowledgments.** This work was supported by the California Regional PM<sub>10</sub>/PM<sub>2.5</sub> Air Quality Study (CRPAQS) Agency under the management of the California Air Resources Board and by the U.S. Environmental Protection Agency under contract R-82805701 for the Fresno Supersite.

## References

- Andrews, E., P. Saxena, S. Musarra, L. M. Hildemann, P. Koutrakis, P. H. McMurry, I. Olmez, and W. H. White (2000), Concentration and composition of atmospheric aerosols from the 1995 SEAVS experiment and a review of the closure between chemical and gravimetric measurements, *J. Air Waste Manage. Assoc.*, *50*(5), 648–664.
- Ashbaugh, L. L., C. E. McDade, W. H. White, P. Wakabayashi, J. L. Collett, and Y. Xiao-Ying (2004), Efficiency of IMPROVE network denuders for removing nitric acid, paper presented at Regional and Global Perspectives on Haze: Causes, Consequences and Controversies—Visibility Specialty Conference, Air and Waste Manage. Assoc., Asheville, N. C., 25–29 Oct.
- Atkinson, R., A. M. Winer, and J. N. Pitts Jr. (1986), Estimation of nighttime N<sub>2</sub>O<sub>5</sub> concentrations from ambient NO<sub>2</sub> and NO<sub>3</sub> radical concentrations and the role of N<sub>2</sub>O<sub>5</sub> in night-time chemistry, *Atmos. Environ.*, *20*(2), 331–339.
- Baldauf, R. W., D. D. Lane, G. A. Marotz, and R. W. Wiener (2001), Performance evaluation of the portable MiniVol particulate matter sampler, *Atmos. Environ.*, *35*, 6087–6091.
- Barber, C. B., D. P. Dobkin, and H. T. Huhdanpaa (1996), The quickhull algorithm for convex hulls, *Trans. Math. Software*, *22*(4), 469–483.
- California Air Resources Board (2004), Climate change emissions inventory, draft report, Calif. Environ. Prot. Agency Air Resour. Board, Sacramento, Calif.
- Chan, C. K., R. C. Flagan, and J. H. Seinfeld (1992), Water activities of NH<sub>4</sub>NO<sub>3</sub>/(NH<sub>4</sub>)<sub>2</sub>SO<sub>4</sub> solutions, *Atmos. Environ. Part A*, *26*, 1661–1673.
- Chen, L.-W. A., B. G. Doddridge, R. R. Dickerson, J. C. Chow, and R. C. Henry (2002), Origins of fine aerosol mass in the Baltimore-Washington corridor: Implications from observation, factor analysis, and ensemble air parcel back trajectories, *Atmos. Environ.*, *36*(28), 4541–4554.
- Chen, L.-W. A., J. C. Chow, J. G. Watson, H. Moosmüller, and W. P. Arnott (2004), Modeling reflectance and transmittance of quartz-fiber filter samples containing elemental carbon particles: Implications for thermal/optical analysis, *J. Aerosol Sci.*, *35*(6), 765–780, doi:10.1016/j.jaerosci.2003.12.005.
- Chow, J. C., and J. G. Watson (1999), Ion chromatography in elemental analysis of airborne particles, in *Elemental Analysis of Airborne Particles*, vol. 1, edited by S. Landsberger and M. Creatchman, pp. 97–137, Gordon and Breach, New York.
- Chow, J. C., and J. G. Watson (2002), PM<sub>2.5</sub> carbonate concentrations at regionally representative Interagency Monitoring of Protected Visual Environment sites, *J. Geophys. Res.*, *107*(D21), 8344, doi:10.1029/2001JD000574.
- Chow, J. C., J. G. Watson, D. H. Lowenthal, P. A. Solomon, K. L. Magliano, S. D. Ziman, and L. W. Richards (1992), PM<sub>10</sub> source apportionment in California's San Joaquin Valley, *Atmos. Environ., Part A*, *26*(18), 3335–3354.
- Chow, J. C., J. G. Watson, D. H. Lowenthal, P. A. Solomon, K. L. Magliano, S. D. Ziman, and L. W. Richards (1993a), PM<sub>10</sub> and PM<sub>2.5</sub> compositions in California's San Joaquin Valley, *Aerosol Sci. Technol.*, *18*, 105–128.
- Chow, J. C., J. G. Watson, J. L. Bowen, C. A. Frazier, A. W. Gertler, K. K. Fung, D. Landis, and L. L. Ashbaugh (1993b), A sampling system for reactive species in the western United States, in *Sampling and Analysis of Airborne Pollutants*, edited by E. D. Winegar and L. H. Keith, pp. 209–228, A. F. Lewis, New York.
- Chow, J. C., J. G. Watson, L. C. Pritchett, W. R. Pierson, C. A. Frazier, and R. G. Purcell (1993c), The DRI thermal/optical reflectance carbon analysis system: Description, evaluation and applications in U.S. air quality studies, *Atmos. Environ., Part A*, *27*(8), 1185–1201.
- Chow, J. C., J. G. Watson, D. H. Lowenthal, P. A. Solomon, K. L. Magliano, S. D. Ziman, and L. W. Richards (1994), PM<sub>10</sub> and PM<sub>2.5</sub> chemical characteristics and source apportionment in the San Joaquin Valley, in *Planning and Managing Regional Air Quality, Modeling and Measurement Studies*, edited by P. A. Solomon, pp. 687–698, CRC Press, Boca Raton, Fla.
- Chow, J. C., J. G. Watson, Z. Lu, D. H. Lowenthal, C. A. Frazier, P. A. Solomon, R. H. Thuillier, and K. L. Magliano (1996), Descriptive analysis of PM<sub>2.5</sub> and PM<sub>10</sub> at regionally representative locations during SJVAQS/AUSPEX, *Atmos. Environ.*, *30*(12), 2079–2112.
- Chow, J. C., J. G. Watson, D. H. Lowenthal, R. Hackney, K. L. Magliano, D. Lehrman, and T. B. Smith (1998), Temporal variations of PM<sub>2.5</sub>, PM<sub>10</sub>, and gaseous precursors during the 1995 Integrated Monitoring Study in central California, in *Proceedings of PM<sub>2.5</sub>: A Fine Particle Standard*, edited by J. C. Chow and P. Koutrakis, pp. 59–77, Air and Waste Manage. Assoc., Pittsburgh, Pa.
- Chow, J. C., J. G. Watson, D. H. Lowenthal, R. Hackney, K. L. Magliano, D. Lehrman, and T. Smith (1999), Temporal variations of PM<sub>2.5</sub>, PM<sub>10</sub>, and gaseous precursors during the 1995 Integrated Monitoring Study in central California, *J. Air Waste Manage. Assoc.*, *49*(PM), PM16–PM24.
- Chow, J. C., J. G. Watson, D. Crow, D. H. Lowenthal, and T. M. Merrifield (2001), Comparison of IMPROVE and NIOSH carbon measurements, *Aerosol Sci. Technol.*, *34*(1), 23–34.
- Chow, J. C., J. G. Watson, L.-W. A. Chen, W. P. Arnott, H. Moosmüller, and K. K. Fung (2004), Equivalence of elemental carbon by thermal/optical reflectance and transmittance with different temperature protocols, *Environ. Sci. Technol.*, *38*(16), 4414–4422.
- Chow, J. C., J. G. Watson, L.-W. A. Chen, G. Paredes-Miranda, M. C. Chang, D. Trimble, K. K. Fung, J. Zhang, and J. Z. Yu (2005a), Refining temperature measures in thermal/optical carbon analysis, *Atmos. Chem. Phys.*, *5*, 4477–4505.
- Chow, J. C., J. G. Watson, D. H. Lowenthal, and K. Magliano (2005b), Loss of PM<sub>2.5</sub> nitrate from filter samples in central California, *J. Air Waste Manage. Assoc.*, *55*(8), 1158–1168.
- Chow, J. C., J. G. Watson, D. H. Lowenthal, L.-W. A. Chen, R. J. Tropp, K. Park, and K. Magliano (2006a), PM<sub>2.5</sub> and PM<sub>10</sub> mass measurements in California's San Joaquin Valley, *Aerosol Sci. Technol.*, in press.
- Chow, J. C., J. G. Watson, D. H. Lowenthal, L.-W. A. Chen, and K. Magliano (2006b), Particulate carbon measurements in California's San Joaquin Valley, *Chemosphere*, *62*(3), 337–348.
- Chow, J. C., J. G. Watson, L.-W. A. Chen, D. Koracin, B. Zielinska, D. Tang, F. Perera, J. J. Cao, and S. C. Lee (2006c), Exposure to PM<sub>2.5</sub> and PAHs from the Tong Liang, China, epidemiological study, *J. Environ. Sci. Health, Part A*, *41*, 517–542, doi:10.1080/10934520600564253.
- El-Zanan, H. S., D. H. Lowenthal, B. Zielinska, J. C. Chow, and N. Kumar (2005), Determination of the organic aerosol mass to organic carbon ratio in IMPROVE samples, *Chemosphere*, *60*(4), 485–496.
- Fine, P. M., G. R. Cass, and B. R. T. Simoneit (2002), Organic compounds in biomass smoke from residential wood combustion: Emissions characterization at a continental scale, *J. Geophys. Res.*, *107*(D21), 8349, doi:10.1029/2001JD000661.
- Green, M. C., R. G. Flöcchini, and L. O. Myrup (1992), The relationship of the extinction coefficient distribution to wind field patterns in southern California, *Atmos. Environ., Part A*, *26*(5), 827–840.
- Grosjean, D., and S. K. Friedlander (1975), Gas-particle distribution factors for organic and other pollutants in the Los Angeles atmosphere, *J. Air Pollut. Control Assoc.*, *25*(10), 1038–1044.
- Hering, S. V., and G. R. Cass (1999), The magnitude of bias in the measurement of PM<sub>2.5</sub> arising from volatilization of particulate nitrate from Teflon filters, *J. Air Waste Manage. Assoc.*, *49*(6), 725–733.
- Khlystov, A., C. O. Stanier, S. Takahama, and S. N. Pandis (2005), Water content of ambient aerosol during the Pittsburgh Air Quality Study, *J. Geophys. Res.*, *110*(D7), D07S10, doi:10.1029/2004JD004651.
- Lehrman, D. E., T. B. Smith, and W. R. Knuth (1998), California Regional PM<sub>10</sub>/PM<sub>2.5</sub> Air Quality Study (CRPAQS) 1995 integrated monitoring study data analysis: Work element 2.2.2—Meteorological representativeness and work element 2.2.3—Fog and low clouds characteristics, T&B Syst., Santa Rosa, Calif.
- Louie, P. K. K., J. C. Chow, L.-W. A. Chen, J. G. Watson, G. Leung, and D. Sin (2005), PM<sub>2.5</sub> chemical composition in Hong Kong: Urban and regional variations, *Sci. Total Environ.*, *338*(3), 267–281.
- Magliano, K. L., A. J. Ranzieri, and P. A. Solomon (1998a), Chemical mass balance modeling of the 1995 Integrated Monitoring Study database, in *Proceedings of PM<sub>2.5</sub>: A Fine Particle Standard*, edited by J. C. Chow and P. Koutrakis, pp. 824–838, Air and Waste Manage. Assoc., Pittsburgh, Pa.
- Magliano, K. L., A. J. Ranzieri, P. A. Solomon, and J. G. Watson (1998b), Chemical mass balance modeling of data from the 1995 Integrated Monitoring Study, Calif. Air Resour. Board, Sacramento, Calif.
- Magliano, K. L., V. M. Hughes, L. R. Chinkin, D. L. Coe, T. L. Haste, N. Kumar, and F. W. Lurmann (1999), Spatial and temporal variations in PM<sub>10</sub> and PM<sub>2.5</sub> source contributions and comparison to emissions during the 1995 Integrated Monitoring Study, *Atmos. Environ.*, *33*(29), 4757–4773.

- Malm, W. C., J. F. Sisler, D. Huffman, R. A. Eldred, and T. A. Cahill (1994), Spatial and seasonal trends in particle concentration and optical extinction in the United States, *J. Geophys. Res.*, *99*(D1), 1347–1370.
- Mochida, M., and K. Kawamura (2004), Hygroscopic properties of levoglucosan and related organic compounds characteristic to biomass burning aerosol particles, *J. Geophys. Res.*, *109*, D21202, doi:10.1029/2004JD004962.
- Moya, M., A. S. Ansari, and S. N. Pandis (2001), Partitioning of nitrate and ammonium between the gas and particulate phases during the 1997 IM-ADA-AVER study in Mexico City, *Atmos. Environ.*, *35*(10), 1791–1804.
- Poore, M. W. (2002), Levoglucosan in PM<sub>2.5</sub> at the Fresno Supersite, *J. Air Waste Manage. Assoc.*, *52*(1), 3–4.
- Pun, B. K., and C. Seigneur (2001), Sensitivity of particulate matter nitrate formation to precursor emissions in the California San Joaquin Valley, *Environ. Sci. Technol.*, *35*(14), 2979–2987.
- Rees, S. L., A. L. Robinson, A. Khlystov, C. O. Stanier, and S. N. Pandis (2004), Mass balance closure and the federal reference method for PM<sub>2.5</sub> in Pittsburgh, Pennsylvania, *Atmos. Environ.*, *38*(20), 3305–3318.
- Rinehart, L. R., E. M. Fujita, J. C. Chow, K. Magliano, and B. Zielinska (2006), Spatial distribution of PM<sub>2.5</sub> associated organic compounds in central California, *Atmos. Environ.*, *40*(2), 290–303.
- Russell, L. M. (2003), Aerosol organic-mass-to-organic-carbon ratio measurements, *Environ. Sci. Technol.*, *37*(13), 2982–2987, doi:10.1021/es026123w.
- Sandwell, D. T. (1987), Biharmonic spline interpolation of GEOS-3 and SEASAT altimeter data, *Geophys. Res. Lett.*, *2*, 139–142.
- Schauer, J. J., and G. R. Cass (2000), Source apportionment of wintertime gas-phase and particle-phase air pollutants using organic compounds as tracers, *Environ. Sci. Technol.*, *34*(9), 1821–1832.
- Seinfeld, J. H., and S. N. Pandis (1998), *Atmospheric Chemistry and Physics: From Air Pollution to Climate Change*, John Wiley, Hoboken, N. J.
- Simoneit, B. R. T. (2002), Chemical characterization of sub-micron organic aerosols in the tropical trade winds of the Caribbean using gas chromatography-mass spectrometry, *Atmos. Environ.*, *36*(33), 5259–5263.
- Simoneit, B. R. T., J. J. Schauer, C. G. Nolte, D. R. Oros, V. O. Elias, M. P. Fraser, W. F. Rogge, and G. R. Cass (1999), Levoglucosan, a tracer for cellulose in biomass burning and atmospheric particles, *Atmos. Environ.*, *33*(2), 173–182.
- Smith, T. B., and D. E. Lehrman (1994), Long-range tracer studies in the San Joaquin Valley, in *Proceedings of Regional Photochemical Measurement and Modeling Studies*, vol. 1, edited by A. J. Ranzieri and P. A. Solomon, pp. 151–165, Air and Waste Manage. Assoc., Pittsburgh, Pa.
- Stockwell, W. R., J. G. Watson, N. F. Robinson, W. Steiner, and W. W. Sylte (2000), The ammonium nitrate particle equivalent of NO<sub>x</sub> emissions for wintertime conditions in central California's San Joaquin Valley, *Atmos. Environ.*, *34*(27), 4711–4717.
- Subramanian, R., A. Y. Khlystov, J. C. Cabada, and A. L. Robinson (2004), Positive and negative artifacts in particulate organic carbon measurements with denuded and undenuded sampler configurations, *Aerosol Sci. Technol.*, *38*, suppl. 1, 27–48.
- Takahama, S., A. E. Wittig, D. V. Vayenas, C. I. Davidson, and S. N. Pandis (2004), Modeling the diurnal variation of nitrate during the Pittsburgh Air Quality Study, *J. Geophys. Res.*, *109*, D16S06, doi:10.1029/2003JD004149.
- Turpin, B. J., and H. J. Lim (2001), Species contributions to PM<sub>2.5</sub> mass concentrations: Revisiting common assumptions for estimating organic mass, *Aerosol Sci. Technol.*, *35*(1), 602–610.
- Turpin, B. J., J. J. Huntzicker, and S. V. Hering (1994), Investigation of organic aerosol sampling artifacts in the Los Angeles basin, *Atmos. Environ.*, *28*(19), 3061–3071.
- U.S. Environmental Protection Agency (1997), National ambient air quality standards for particulate matter: Final rule, *Fed. Regist.*, *62*(138), 38,651–38,701.
- Watson, J. G., and J. C. Chow (2002a), A wintertime PM<sub>2.5</sub> episode at the Fresno, CA Supersite, *Atmos. Environ.*, *36*(3), 465–475.
- Watson, J. G., and J. C. Chow (2002b), Comparison and evaluation of in situ and filter carbon measurements at the Fresno Supersite, *J. Geophys. Res.*, *107*(D21), 8341, doi:10.1029/2001JD000573.
- Watson, J. G., J. C. Chow, Z. Lu, E. M. Fujita, D. H. Lowenthal, and D. R. Lawson (1994), Chemical mass balance source apportionment of PM<sub>10</sub> during the Southern California Air Quality Study, *Aerosol Sci. Technol.*, *21*(1), 1–36.
- Watson, J. G., P. J. Lioy, and P. K. Mueller (1995), The measurement process: Precision, accuracy, and validity, in *Air Sampling Instruments for Evaluation of Atmospheric Contaminants*, 8th ed., edited by B. S. Cohen and S. V. Hering, pp. 187–194, Am. Conf. of Govt. Ind. Hyg., Cincinnati, Ohio.
- Watson, J. G., D. W. DuBois, R. DeMandel, A. P. Kaduwela, K. L. Magliano, C. McDade, P. K. Mueller, A. J. Ranzieri, P. M. Roth, and S. Tanrikulu (1998), Field program plan for the California Regional PM<sub>10</sub>/PM<sub>2.5</sub> Air Quality Study (CRPAQS), Desert Res. Inst., Reno, Nev.
- Watson, J. G., J. C. Chow, J. L. Bowen, D. H. Lowenthal, S. Hering, P. Ouchida, and W. Oslund (2000), Air quality measurements from the Fresno Supersite, *J. Air Waste Manage. Assoc.*, *50*(8), 1321–1334.
- Watson, J. G., J. C. Chow, D. H. Lowenthal, M. R. Stolzenburg, N. M. Kreisberg, and S. V. Hering (2002), Particle size relationships at the Fresno Supersite, *J. Air Waste Manage. Assoc.*, *52*(7), 822–827.
- White, W. H., and P. T. Roberts (1977), On the nature and origins of visibility-reducing aerosols in the Los Angeles air basin, *Atmos. Environ.*, *11*(9), 803–812.
- Zhang, X. Q., and P. H. McMurry (1987), Theoretical analysis of evaporative losses from impactor and filter deposits, *Atmos. Environ.*, *21*(8), 1779–1789.
- Zhang, X. Q., and P. H. McMurry (1992), Evaporative losses of fine particulate nitrates during sampling, *Atmos. Environ., Part A*, *26*(18), 3305–3312.

L.-W. A. Chen, J. C. Chow, D. H. Lowenthal, and J. G. Watson, Division of Atmospheric Sciences, Desert Research Institute, Reno, NV 89512, USA. (judy.chow@dri.edu)

D. E. Lehrman, Technical and Business Systems, Santa Rosa, CA 95404, USA.

K. A. Magliano and K. Turkiewicz, California Air Resources Board, Sacramento, CA 95812, USA.